THESIS

DEVELOPMENT OF A NITRIC OXIDE MEASUREMENT METHOD IN TISSUE MEDIA

Submitted by

Cherelle M. Bishop

Department of Chemistry

In partial fulfillment of the requirements

For the Degree of Master of Science

Colorado State University

Fort Collins, Colorado

Spring 2012

Master's Committee:

Advisor: Melissa Reynolds

Charles Henry
Stuart Tobet

ABSTRACT

DEVELOPMENT OF A NITRIC OXIDE MEASUREMENT METHOD IN TISSUE MEDIA

Nitric oxide (NO) is involved in many biological pathways such as vasodilatation and cellular migration. The biological roles of NO have been most heavily investigated using cell and tissue culture models. The limitations with current analytical measurement methods used most commonly with these studies, however, are that they often do not record in real-time or measure NO directly. This makes it difficult to understand the concentration dependent response activity of NO. To overcome these limitations, a measurement method has been developed that enables the real-time measurement of NO in buffered tissue media (pH 7.4, buffered with CO_2 gas, 37 °C). The design of our system included multi-volume custom sample cells with a pH probe and multiple gas supply inputs, a flow regulated CO_2 gas system and a chemiluminescence detector. Results demonstrated the expected first–order NO release kinetics using a model NO donor (MAHMA/NO) in phosphate buffered saline (PBS) over a specified volume range. The following half-lives were found: 63±2 s (2 mL), 65±2 s (6 mL), 63±4 s (8 mL) and 67±9 s (10 mL). Using this method at these buffer volumes, an experiment was conducted using 11 mM MAHMA/NO stock used to demonstrate that NO release was linearly proportional with respect to buffer volume with a linear fit of R^2=0.9936. The linearity of NO release allowed NO release measurements of 4.4 x10^{-7} M MAHMA/NO concentration in 10 mL PBS achieving NO recovery of 117±2 and MAHMA/NO

decomposition half-lives 66±2. The analysis of a 10^{-7} M MAHMA/NO was not measurable previously using other chemiluminescence methods.

Subsequent results in tissue media buffered with 5% CO_2 at a controlled rate of 20 mL/min showed statistically similar kinetic rates 68±5 s (2 mL) to that of the PBS, demonstrating the ability to measure NO in real time under tissue conditions. The simultaneous pH measurements confirmed that the pH was constant at 7.4 during the NO release portion of the experiment, an important aspect to maintain accurate kinetics. Using this method for NO release measurement in tissue media, another NO donor, DETA/NO, was used to look at steady-state release for 1.5 h. The total NO release was 0.12±0.02 (nmol) and the NO release rate was 22±3 (fmol/s). This is the first analytical measurement method that enables detection of NO release from NO donors in buffered tissue media method mimicking *in vitro* condition.

ACKNOWLEDGEMENTS

First and foremost, I would be lost without my Lord and Savior Jesus Christ, whose been my rock and seen me through everything the past year. I am so grateful for my parent's endless encouragement and unwavering support over the last few years. Padre, I am thankful that through graduate school, I am able to share so much more of my research experience with you and talk about recent literature. Madre, I am so thankful for your support and love. Brothers, thank you for believing in me and rooting for me. Grandma, thank you for all the cards, prayers and support, it meant so much.

I would like to thank my advisor, Dr. Melissa Reynolds, for supporting me and helping me grow as a chemist. I am grateful for her allowing me to work on a project to develop novel measurement methods for nitric oxide, which is a molecule that has great potential to influence treatment of many ailments and diseases in the future. I am grateful for the support of the Therapeutic Material and Biointerfacial Research (TMBR) group, who assisted me in the completion of this research project. I would like to especially thank Jessica Joslin for several great conversations on the state of my research when I really needed feedback.

I would also like to thank the members of my thesis committee, Dr. Chuck Henry and Dr. Stuart Tobet. I am thankful that through the Gk-12 project I have been able to understand your research goal and get to know both of you. Chuck, I am grateful that you always made time to sit down and talk with me during my time here at Colorado State University.

Also, to everyone involved with GK-12 Colorado High-Education Interdisciplinary Project (CHIP) project, I am so thankful to have been a part of integrating science, education and research to further understand cellular communication. I would specifically like to thank Matt Stratton from many in-depth conversations on how tissue media is used in cellular migration experiments and biological approaches that were invaluable to the development of this method. I have learned a lot about how to communicate science across disciplines and learned a great deal from transferring my research into K-12 classroom. I would like to thank my mentor teacher, Kate McDonnell, for being flexible in allowing research and our educational goals to work towards the completion of this thesis and an education publication.

I would like to thank my Fort Collins family including: Megan & Monika Easterly, Bill & Cindie Williams and the Meadowlark Church of Christ. These people have kept me sane the past few months as I wrote this up. To the many people, who helped with thesis correction, I would like to thank: Melissa Reynolds, Gary Bishop, Annette Bishop, Jen Blaser, Katie Altmiller, Kate Wold, Megan Easterly, Lisa Lee Mellmann and Jaclyn Adkins.

TABLE OF CONTENTS

Page No.

ABSTRACT…… ii

ACKNOWLEDGEMENTS…… iv

LISTS OF TABLES……....ix

LIST OF FIGURES…….x

LIST OF ACRONYMS AND ABBREVIATIONS……...xiv

CHAPTER

1. INTRODUCTION…….1

1.1 Biological Impact of NO……...2

1.2 Synthesis of NO *in vivo*…….....6

1.3 Secondary Signaling Pathways of NO……..9

1.4 Nitric Oxide's Role in Central Nervous System as a Neurotransmitter……11

1.5 Nitric Oxide Hypothesized Role in Cell Migration……..15

1.6 Classes of NO Donors……..15

1.7 Nitric Oxide Detection Methods…….....19

1.8 Summary…….....27

1.9 Reference…….....30

2. METHOD DEVELOPMENT TO MEASURE NO FROM LOWER CONCENTRATION OF NO DONOR SOLUTIONS BY CHEMILUMINESCENCE DETECTION……36

2.1 Introduction……..36

2.2 Materials……...37

2.3 Methods……37

2.3.1 Nitric Oxide Donor Synthesis…… .37

2.3.2 Nitric Oxide Release Measurements…….38

2.4 Results…….40

2.4.1 Current state of Chemiluminescence Methodology……...40

2.4.2 Nitric Oxide Release from 10^{-4} M MAHMA/NO Decomposition Experiments in 2 mL ……. ……....42

2.4.3 Nitric Oxide Release from 10^{-4} M MAHMA/NO Decomposition Experiments in 6, 8 and 10 mL……..45

2.4.4 Nitric Oxide Release from 10^{-7} M MAHMA/NO Decomposition Experiments in 10 mL……....52

2.5 Conclusions……..54

2.6 References……55

3. MEHTOD TO QUANTIFY NO DELIVERY FROM NO DONOR CONCENTRATION IN A CARBON DIOXIDE BUFFERED TISSUE MEDIA SOLUTION……56

3.1 Introduction……..56

3.2 Materials……...57

3.3 Methods……57

3.3.1 Nitric Oxide Donor Synthesis……..….57

3.3.2 Real-time pH measurements ……....57

3.3.3 Tissue Media Preparation…….....60

3.3.4 Nitric Oxide Release Measurements…….....60

3.4 Results……..61

3.4.1 Method Optimization to enable NO Release from MAHMA/NO Decomposition in Buffered Tissue Media…….61

3.4.2 Nitric Oxide Release from 10^{-4} M MAHMA/NO Decomposition Experiments in Buffered Tissue Media……65

3.4.3 Nitric Oxide Release from DETA/NO Decomposition in Buffered Tissue Media……69

3.5 Conclusions…… 72

3.6 References……73

4. FUTURE DIRECTIONS……74

4.1 Future Directions……..74

4.2 References…… 81

LISTS OF TABLES

TABLE

1.1 Effect of NO on cGMP Levels in Various Tissue……...9

1.2 Common Biological Interferences in Electrochemical Detection of NO……....22

2.1 Flow Table for Air for 150 mm Flow Meters with Aluminum Ball……..…48

2.2 Summary of 10^{-4} M MAHMA/NO Decomposition in Different Volumes of PBS……..……...49

3.1 Acid and Base Titration Injection Volumes……...59

3.2 Evaluating the Function of 3-port Sample Cell to the 2-port Sample Cell by Comparing Experimentally Derived MAHMA/NO Half-Lives…..…….. 64

3.3 Evaluating the Difference in Aqueous Environments on MAHMA/NO Half-Lives and NO Recovery at pH 7.40 and 37 °C…….…….……67

LISTS OF FIGURES

FIGURE

1.1 Nitric oxide is an important signaling molecule involved in many biological processes and cellular responses *in vivo*……..…..1

1.2 The conversion of L-arginine to L-citrulline by nitric oxide synthase (NOS) with the addition of varies cofactors, nicotinamide adenine dinucleotide phosphate (NADPH) and oxygen to produce NO *in vivo*…….…… ……7

1.3 In the cardiovascular system, NO influences many biological pathways including inhibiting platelet activation, angiogenesis and vasodilatation through smooth muscle relaxation. ……..10

1.4 A drawing of a synapse between the axon terminal and the postsynaptic cell that illustrates all the steps involved in neurotransmission. All important features discussed have been labeled……...……11

1.5 A drawing of a synapse that produces NO and leads to many cellular responses……...14

1.6 Above are 6 molecules each from different classes of NO donors: organic nitrates, *S*-nitrosothiols, organic nitrites, diazeniumdiolates, metal-NO compounds and oximes……...….16

1.7 The chemical structures of MAHMA/NO (left) and DETA/NO (right) are shown above. Both compounds are diazeniumdiolates, a class of NO donors…….18

1.8 An expression for the 2 electron reduction of NO at negative potential in electro-reduction detection systems for NO…….…....21

1.9 An expression for the 3 electron oxidation of NO at positive potential in electro-oxidation detection systems for NO……...21

1.10 An expression explaining how NO or any radical of interest (R*) is trapped by reacting with a species (ST) that traps the radical quickly to create a more stable radical trap addict (R*-SA)…… .23

1.11 An expression explaining how NO is detected using chemiluminescence.…25

1.12 Flow chart showing the experimental development of custom method based on MAHMA/NO decomposition……..28

2.1 A diagram of the NO release measurement set-up with bubble and flow gas entrances (gas regulation), the injection port (sample) and gas removal port (reaction chamber) all labeled…….42

2.2 The first order rate law expression for MAHMA/NO decomposition……...43

2.3 The decomposition reaction for MAHMA/NO in aqueous solution at pH 7.4, 37 °C. Based on literature precedent, the rate of reaction has been documented to be k= 0.0116 giving a 60 s half-life for MAHMA/NO…..…43

2.4 Typical NO release profile for MAHMA/NO decomposition (A, left). NO release measurements were converted into ln($[MAHMA/NO]_{decomp}$) using first order kinetics to calculate accurate MAHMA/NO half-lives (B, right)……..……...45

2.5 As the buffer volume increase from 2 mL to 6 mL the increase in volume allows more NO to be soluble in the buffer, trapping NO and artificially slowing the experimentally derived MAHMA/NO half-lives…...47

2.6 Experimental half-lives for MAHMA/NO at different volumes of PBS buffer relative to the literature value for MAHMA/NO, 60 s (solid line)……50

2.7 The graph shows the average moles of NO released at five different volume of PBS using an 11 mM MAHMA/NO stock. Using a linear regression, the data was fitted achieving a linear fit of $R^2 = 0.9936$…….....51

2.8 Even at more dilute concentration of NO donor, the NO release profile for MAHMA/NO decomposition is conserved although short lived at 500s (left, A). The rate constant determination graph shows rate constant determination using first order kinetics to obtain accurate MAHMA/NO half-lives (right, B)…….52

2.9 A direct comparison of the NO release profiles (moles NO) for the 10^{-4} M MAHMA/NO (A) and 10^{-7} M MAHMA/NO (B)…….54

3.1 A diagram of the NO release measurement set-up with the 3-port custom NOA sample cell with the bubble and flow gas entrances (gas regulation), the injection port (sample), gas removal port (reaction chamber) and the pH probe port all labeled.....58

3.2 A comparison of the standard 2-port small volume NOA cell (left, A) and the custom 3-port in two sizes, small volume NOA cell (center, B) and large volume NOA cell (left, C)……..63

3.3 A graph shows the real-time pH response of the pH probe following different injection volumes of 0.1 M NaOH (blue) and 0.1 M HCl (red)…..65

3.4 This figure shows the average pH response for addition of 5% carbon dioxide at 20 mL/min to the tissue media. After 1.6 h, 20 µl of 11 mM MAHMA/NO solution was injected and NO release is observed from …MAHMA/NO decomposition…….68

3.5 The decomposition reaction for DETA/NO in aqueous solution at pH 7.4,37 °C……..……..69

3.6 This figure shows the average pH response following a 20 µl injection of 60 mM DETA/NO and the NO release profile from DETA/NO decomposition for 1.5 hr……...…..71

4.1 A direct comparison of the NO release profile (moles NO) for the 10^{-7} M MAHMA/NO in buffered tissue (A) and 10^{-7} M MAHMA/NO in PBS (B)……..……..…76

LIST OF ACRONYMS AND ABBREVIATIONS

NO	Nitric Oxide
ERDF	Endothelium-derived relaxing factor
GC	Guanlylate cyclase
cGMP	Cyclic guanosine monophosphate
L-NMMA	N^{ω}-monomethyl-L-argine
GABA	Gamma amino butyric acid
NOS	Nitric oxide synthase
NADPH	Nicotinamide adenine dinucleotide phosphate
eNOS	Endothelial nitric oxide synthase
nNOS	Neuronal nitric oxide synthase
iNOS	Inducible nitric oxide synthase
GTP	Guanosine 5'-triphosphate
GSNO	*S*-Nitrosoglutathione
DEA/NO	Diethylamine diazeniumdiolate
SNP	Sodium Nitroprusside
NOR-3	(+/-)-(E)-ethyl-2-[(E)-hydroxyimino]-5-nitro-3-hexeneamide
MAHMA/NO	Methylaminehexylmethylamine diazeniumdiolate
DETA/NO	Diethylenetriamine diazeniumdiolate
NMDA	N-methyl D-aspartate
EPR	Electron paramagnetic resonance

Hb	Hemoglobin
NO_2^*	Excited state nitrogen dioxide species
PBS	Phosphate Buffered Saline
HEPES	4-(2-hydroxyethyl)-1-piperazineethanesulfonic acid
TRIS	Tris(hydroxymethyl)aminomethane
PSI	Pound force per square inch
UV	Ultraviolet
NOA	Nitric Oxide Analyzer
NaOH	Sodium Hydroxide
PPB	Part per billion
CO_2	Carbon dioxide
ID	Inner diameter
OD	Outer diameter
HCl	Hydrochloric acid
DPTA/NO	1-[N-(3Aminopropyl)-N-(3-aminopropyl)]diazen-1-ium-1,2-diolate
O_2	Oxygen
$ONOO^-$	Peroxynitrite

1. *INTRODUCTION*

In the late 1700's Sir Humprey Davy conducted the very first experiment to study the effect of nitric oxide (NO) on respiration. The experiment was ill conceived, where he experienced aspiration pneumonitis and nearly died from inhalation of the gas and stated, 'never design again to attempt so rash an experiment'.[1] In the 1900's until the early 1980's, NO was generally studied as an important gas in the atmosphere because of its role in acid rain, smog and depletion of the ozone layer.[2,3] In 1987, the endothelium-derived relaxing factor (EDRF) was discovered to be NO responsible for vasodilatation.[4,5] This established NO as an important molecule in physiological biology.[6] This discovery, also caused an increased research interest in the chemical and biological effects of NO throughout the 1990's. Since then NO has been shown to be an important signaling molecule in vascular, neuronal and immune response pathways summarized in Figure 1.1.[7]

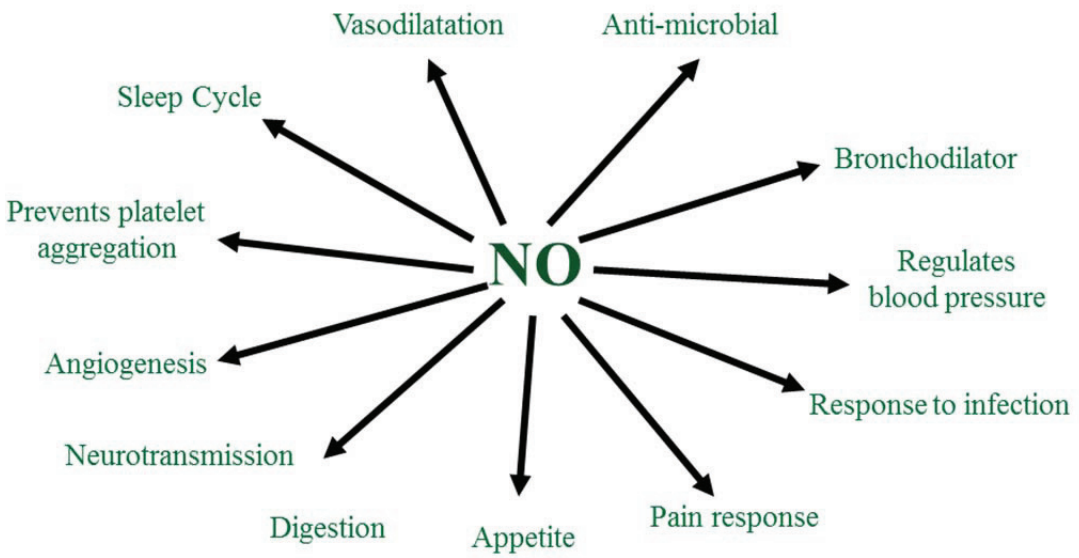

Figure 1.1: Nitric oxide is an important signaling molecule involved in many biological processes and cellular responses *in vivo*.

The significance of NO in biology was recognized by the 1998 Nobel Prize in Physiology and Medicine given to Furchgott, Ignarro and Murad for their work in establishing NO as a chemical signaling agent in physiology.[8,9]

In this introduction, the role of NO in many important biological processes will be discussed. In addition, the use of NO donor compounds to better elucidate the role of NO in cellular processes and the specific analytical techniques used to detect NO release from these compounds will be described. Finally, the rationale for the development of analytical methodologies that allow for the detection of NO in conditions that mirror those of tissue studies will provide the context for this work.

1.1 Biological Impact of NO

Nitric oxide, as an important biological molecule begins with the discovery that NO plays an unique role in the cardiovascular system. Today's understanding of vasodilatation had its roots in the 1970's, where researchers investigated why nitroglycerin was such a powerful heart attack medicine and the mechanism for its biological activity.[10] Murad and colleagues explored these questions by studying how nitroglycerin, nitropusside and NO influenced guanlylate cyclase (GC) activity.[11] Using these sources of NO, NO was found to stimulate a measurable increase in GC in several tissue models. Murad implicated this increase in GC to the presence of NO, a hormone or another endogenous compound; however, this study did not produce concrete experimental evidence to elucidate NO's role in this hypothesis.[12] The experimental evidence strongly suggest that NO was responsible for the increase in GC activity first reported by Ignarro, whose published work demonstrated that oxyhemglobin inhibited endothelium and NO-induced relaxation in bovine intrapulmonary arteries and veins.[4]

This work provided evidence that cyclic guanosine monophosphate (cGMP) levels were elevated by EDRF and demonstrated that the EDRF was NO. Two months later, Palmer independently determined that the EDRF was NO by performing an inhibition study using haemoglobin and a tissue bioassay.[5] Palmer and colleagues were able to state that "the biological activity of the EDRF is accounted for by NO" and served to expand the work presented by Ignarro.[5]

Cardiovascular System:

Twenty-five years have passed since NO was first implicated as the EDRF and demonstrated to be responsible for the vasodilatation of blood vessels. In this time, NO's involvement in the cardiovascular system has been expanded. For example, several studies have been published that demonstrate NO's role in preventing platelet adhesion.[10,13] Furlong showed that anti-platelet adhesion could be inhibited by haemoglobin scavenging of NO, at a binding affinity rate of 10^{15} M^{-1}.[14,15] Additional work showed that NO was largely responsible for blood pressure regulation.[10] Researchers investigated the role of NO in blood pressure by inhibiting NO synthesis using N^{ω}-monomethyl-L-argine (L-NMMA) in both *in vivo* and *in vitro* models of hypertension.[16] This work was further confirmed by a study investigating multi-vascular beds in a rat model, where NO was inhibited through L-NMMA again resulting in the development of hypertension.[17]

Bronchodilation:

Nitric oxide's role is not limited to the cardiovascular system but has also been demonstrated to play an important role in respiration of organisms. Inhalation experiments in guinea pigs demonstrated that NO could serve as a powerful

bronchodilator. In these studies, the animals were exposed to low concentrations of NO gas, and the bronchoconstriction of the animals was reversed.[18] Similar experiments were done independently that served to explain how the bronchodilator response was mediated in the lungs using human tracheal segments harvested from five individuals, who met qualification for heart-lung transplants.[19] This study used the tracheal rings to suggest that nerve cells controlled NO release that induced bronchodilation.[19] Data from these studies showed the controlled inhibition or activation of dilation in bronchi in human lungs. Other work found that NO was present in exhaled air of humans and was shown to be elevated in asthmatic patients.[20,21] This work combined with many others have examined the role of NO and respiration leading to important new developments in asthma treatment and dosaging.[22]

Immune Response:

By the late 1980's and the early 1990's, NO was also implicated in controlling immune response. Nitric oxide was found to be expressed by macrophages and function as a tumoricidal and antimicrobial agent.[7] Investigators, first found that macrophages produced NO as a response to infection.[23,24] Patients suffering from infections ranging from hepatitis, tuberculosis, malaria and rheumatoid arthritis expressed NO at higher levels than the control patients.[25] Through experimental studies, NO donor molecules were used to demonstrate the validity that NO has a strong anti-microbial activity *in vivo*. NO releasing compounds were shown to successfully inhibit or kill microbes and the anti-microbial activity of NO was demonstrated to be effective against viruses, bacteria, fungi and parasites.[26] Several studies have found that NO synthesis is not limited to macrophages, but is produced in many other cell lines including phagocytes,

dendritic, natural killer and T and B cells. The production of NO within these cell lines supports its role in immune response.

Central Nervous System:

In the central nervous system, NO has been implicated to influence the perception of pain and the control of sleep, hunger, body temperature and neurosection of hormones.[27] Based on the work of several studies, NO is hypothesized to play a part in how the central nervous system processes pain.[28] The relationship between NO and the pain receptor, nociceptor; however, is not fully understood at this time.[29] Holthusen et al. investigated the direct relationship between NO and pain perception by injecting volunteers with varying amounts of NO dissolved in phosphate buffer and correlating the injection with a pain response.[29] These researchers found that when a 12 nmol dose of NO was injected directly into volunteers, it always induced a pain responds in the volunteer. Zhang et al. demonstrated that NO production occurred within the primary sensory neurons in rats, linking NO to localized tenderness called hyperalgesic pain.[30,31]

The regulation of the sleep-wake cycle is considered to be influenced by NO based on observable changes to the cycle following NO inhibition experiments and infusions of NO donor molecules in mouse and cat models.[32] As with the vasodilatation effect of NO in blood vessels, the release of NO from nerve cells induces smooth muscle relaxation throughout the gastrointestinal tract. This relaxation allows the esophagus to push food into the stomach, which aids the stomachs to digest large amounts of food without producing pressure fluctuations within the stomach.[33] As well as stimulating digestion, NO has also been shown to influence the appetite in rat, mice and chicken models.[34] In the brain, many biological processes are regulated by NO through

neurosecretion of hormones influencing sleep and stress.[27] Neurosecretion of hormones occur through stimulation from NO because it act as a neurotransmitter, making it an important cellular messenger in the brain. Garthwaite et al. first reported this observation, when receptors in cellebellar cells released NO after being stimulated by glutamate.[35] Later, NO's involvement in promoting the release of neurotransmitters like acetylcholine, noradrenaline and gamma amino butyric acid (GABA) was discovered.[27]

1.2 Synthesis of NO in vivo

Nitric oxide has a wide range of influences within mammals, and in the last decade, the molecule has continued to be studied for its biological effects. Moving forward, the monitoring of NO will become increasingly important as researchers use their knowledge of what NO does to treat aliments caused by NO deficiencies. Before these deficiencies can be addressed, it is important to understand how NO is produced *in vivo* to induce these behavioral changes in organisms.

After Ignarro and Palmer demonstrated that NO was the EDRF, other researchers showed that NO is responsible for a number of crucial biological processes. However, no one understood how this endogenous source of NO was produced *in vivo.* In 1989, Mayer found that endothelial cells produced NO through an enzymes termed nitric oxide synthase (NOS).[36] Dawson and Synder expanded on this finding by demonstrating that NO is produced by one of three isoforms of NOS from L-arginine in a two-step synthesis.[37]

This two-step synthesis NO occurs within endothelial cells by the oxidation of L-arginine to L-citrulline by nitric oxide synthase (NOS) and these reactions are catalyzed by nicotinamide adenine dinucleotide phosphate (NADPH) and oxygen (Figure 1.2).

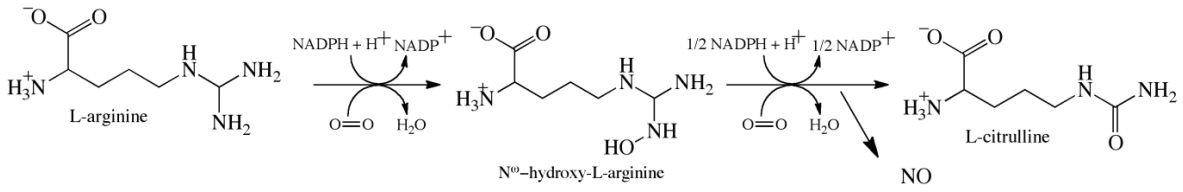

Figure 1.2: The conversion of L-arginine to L-citrulline by nitric oxide synthase (NOS) with the addition of varies cofactors, nicotinamide adenine dinucleotide phosphate (NADPH) and oxygen to produce NO *in vivo*.

NO production *in vivo* is accomplished primarily by NOS, of which there are three main isoforms: endothelial (eNOS), neuronal (nNOS), and inducible (iNOS).[38] The isolation of NOS first came in the brain by work performed by Bredt et al. and was supported by experimental evidence finding NOS in several different cell types including endothelium and neurons.[39,40] After the isolation of nNOS in the brain, the next isoform that was successfully purified was iNOS from a macrophage.[41] The final isoform to be purified was the eNOS from endothelial cells from a bovine aorta which originally stimulated so much of the interest in NO biology and chemistry due to its role in vasodilatation.[42] These three isoforms of NOS are responsible for NO production in different regions of the body and are triggered by different factors. The production of NO from each of these isoform is identical to the synthetic scheme shown in Figure 1.2. These isoforms are found in different cellular hosts, and the cells influence the function that NO serves within these cellular regions.

The endothelial isofom of NOS is principally responsible for producing NO in endothelial cells that line blood vessels. The production of NO in endothelial cells leads to smooth muscle relaxation, which allows for blood flow to be regulated throughout the body. This isoform of NOS was the first to be discovered allowing researchers to begin to understand how endogenous NO was produced.[36] This enzyme is not restricted to vascular endothelium but has since been found in human neuronal cells, astrocytes, t-cells, bone marrow cells, osteoblasts and osteoclasts.[38] The regulation of eNOS is modulated by the phosphorylation, the addition of a phosphate group, and the binding of calcium inducing conformational changes to the enzymes structure to initiate NO production.[38] Additional regulation of eNOS occurs through changes to the shear stress within the blood vessel which can also modulate the enzyme's function.[43]

The neuronal isoform of NOS generates small amounts of NO for chemical signaling within the central nervous system that is associated with pain perception, control of sleep and hunger, and neuronal cell development. The presence of this isoform was first discovered in the brain and since then was found in human lung epithelial cells, testis cells and skin cells. As with eNOS, the neuronal isoform is regulated by calmodulin and calcium. The production of NO is inhibited when these molecules are not bound to the nNOS enzyme.[44]

The inducible NOS is responsible for immune responses in organisms and is involved in controlling anti-microbial, apoptosis and anti-tumor response as a defense against cellular threats. The inducible isoform of NOS, although first isolated in a macrophage and associated with immune response, has also been located in human

hepatocytes, sinusoidal and endothelial cells.[45] Unlike eNOS and nNOS, iNOS is not regulated by calcium because of the tight association of calmodulin.

1.3 Secondary Signaling Pathways of NO

Some of the biological effects attributed to NO result from secondary signaling pathways. The synthesis of NO activated soluble GC increases the production of a secondary signaling molecule, cGMP. This secondary messenger molecule that NO is linked to was confirmed as GC by a series of experiments preformed in Murad's laboratory between 1976 and 1977.[46] Murad et al. connected NO exposure to an increase in the activity of GC in various tissues.[47] The only known receptor for NO is sGC, which governs the conversion of guanosine 5'-triphosphate (GTP) to cGMP.[48] Several studies using various tissue models summarized in Table 1.1, have demonstrate that NO increase the formation of cGMP in various tissues.[46]

Table 1.1: Effect of NO on cGMP Levels in Various Tissue[47]

Tissue	cGMP Formed (pmol/mg min)
Rat liver	30.5
Bovine lung	32.5
Bovine trachael smooth muscle	33.4
Rat cerebral cortex	20.2
Rat heart	23.1
Rat kidney	18.9
Rat skeletal muscle	13.8
Rat spleen	5.2
Rat small intestinal muscle	5.8
Rat adrenal	10.5
Rat epididymal fat	11.5

Understanding secondary signaling pathways is important because they induce secondary effects that impact cellular function. As a secondary messenger cGMP induces a wide-range of cellular processes through the activation of a kinase cascade, which stimulates the cell to regulate the translation or transcription of genes responsible for producing various cellular responses. The sGC cylcle has been implemented in many cellular processes including vasodilatation, angiogenesis, cellular migration and matrix degradation. In the cardiovascular system, for example, NO produces a cascade of secondary signaling molecules that leads to vasodilatation and angiogenesis. The binding of vasoactive or angiogenic factors to surface receptors on endothelial cell activates the synthesis of NO from eNOS and stimulates vasodilatation or angiogenesis. As illustrated in Figure 1.3, NO produced by eNOS diffuses from the endothelial cells into smooth muscle cell inducing relaxation termed vasodilatation. [10]

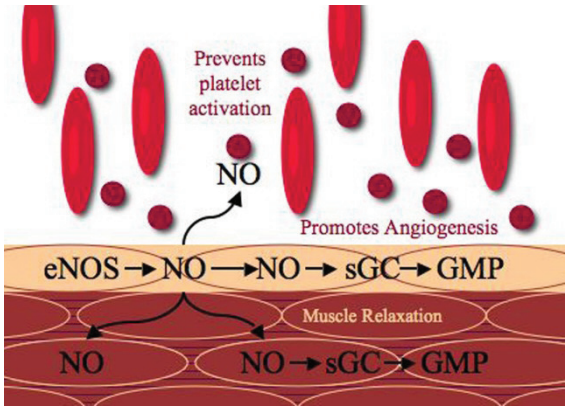

Figure 1.3: In the cardiovascular system, NO influences many biological pathways including inhibiting platelet activation, angiogenesis and vasodilatation through smooth muscle relaxation.

Another secondary effect caused by the production of NO through the activation of soluble GC producing cGMP is angiogenesis. Where the production of cGMP stimulates a kinase cascade that results in the transcription of specific genes leading to cellular responses that cause angiogenesis.[49] Thus, angiogenesis and vasodilatation rely on chemical signaling processes that are activated by NO illustrated in Figure 1.3.

1.4 *Nitric Oxide's Role in Central Nervous System as a Neurotransmitter*

The process of neurotransmission was first proposed by Otto Loewi in 1921, who later went on to discover the very first transmitter, acetylcholine. [50] A simple way to explain neurotransmission is the process in which neurons communicate through electrical and chemical signals to coordinate activity throughout the central nervous system. In general, neurotransmission can be summarized in five steps illustrated in Figure 1.4: 1.Synthesis of neurotransmitter 2.Storage of neurotransmitter 3.Release of neurotransmitter 4.Receptor binding of neurotransmitter and 5.Inactivation of neurotransmitter binding to postsynaptic receptor.[51]

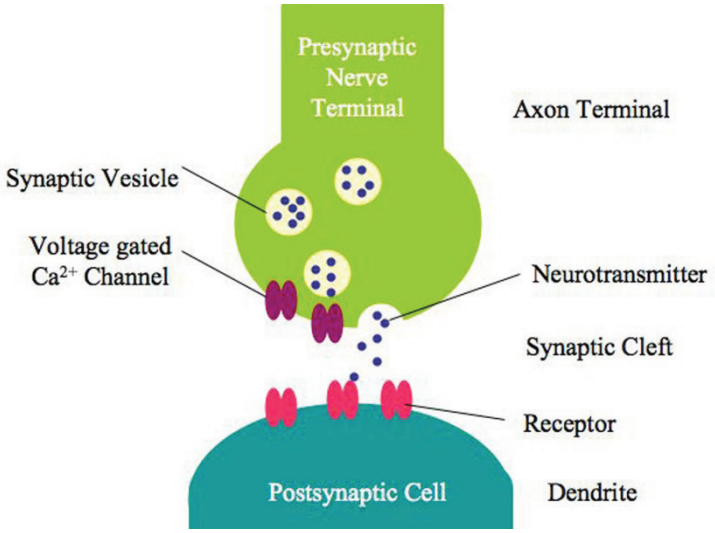

Figure 1.4: A drawing of a synapse between the axon terminal and the postsynaptic cell that illustrates all the steps involved in neurotransmission. All important features discussed have been labeled.

Figure 1.4 shows a cartoon of a synapse between a neuron and a post-synaptic cell, the site for neurotransmission or cellular communication. The synapse allows chemical and electrical signals to be exchanged stimulating a response from the target cell. *Step 1.* The first step requires that the neurotransmitters must be synthesized within the neuron. The necessary enzymes and cofactors must be readily available. *Step 2.* Following synthesis, the neurotransmitters are stored within a synaptic vesicle that is formed in the presynaptic nerve shown in Figure 1.4. *Step 3.* This vesicle moves the neurotransmitter to the presynaptic membrane and releases it following a calcium regulated action potential. When these neurotransmitters are released from the presynaptic membrane into the synaptic cleft (Figure 1.4) the process is termed exocytosis. *Step 4.* The neurotransmitters locate and bind to membrane bound receptors in the post-synaptic cell (Figure 1.4). There are two classes of receptors: metabotropic or ionotropic receptors, which neurotransmitters can selectively bind to influence cellular responses within the target cell. Metabotropic receptors can influence cellular function through the G proteins (i.e. cGMP). Iontropic receptors control either ion channels that are either gated by a ligand or a voltage. Step 5. A termination step is included to allow the nerve to inhibit and terminate the neurotransmission. Termination of the signal is accomplished by the diffusion, destruction or reuptake of the neurotransmitter. This step is important because if transmission continued for sustained periods of time, serious problems could arise from tetanus in muscles and seizures in neurons.

In general, neurotransmitters are classified by their production in the presynaptic nerve, followed by their release into the chemical synapse and their binding to a specific receptor in the post-synaptic cells.[51] Currently there are roughly 100 identified

neurotransmitters and each of these transmitters is in one of two categories: excitatory or inhibitory transmitters. Excitatory transmitters increase the chances that the transmitter will stimulate the nerve to fire an action potential. Inhibitory transmitters suppress nerve from firing allowing signaling to be terminated. Several important amino acid transmitters are: glutamate, aspartate, glycine and GABA.

The idea that NO is a neurotransmitter goes against much of the classical definition of what constitutes a transmitter. The idea that NO was involved in the chemical signaling pathways in the brain was first suggested when NO was found to be present in neurons. The release of glutamate from presynaptic nerve terminals acted upon NMDA receptors, allowing calcium to enter through gated channels into post-synaptic cells.[35] The calcium initiated synthesis of NO from nNOS was shown to induce vasodilatation and increase in cGMP levels. The role of NO in the brain to regulate and influence many cellular processes has allowed some researchers to reason that NO is, in fact, a neurotransmitter capable of influencing cellular signaling in the brain.

NO is known to diffuse through the synaptic cleft and there is evidence that NO influences the regulation of many cellular pathways through the activation and production of cGMP, an important secondary signaling molecule (Figure 1.5). Although it is certain that cGMP is active in modulating cellular activity in the brain, it not completely understood the exact functions that are triggered through these secondary signal in the brain as readily as the cardiovascular system.[37]

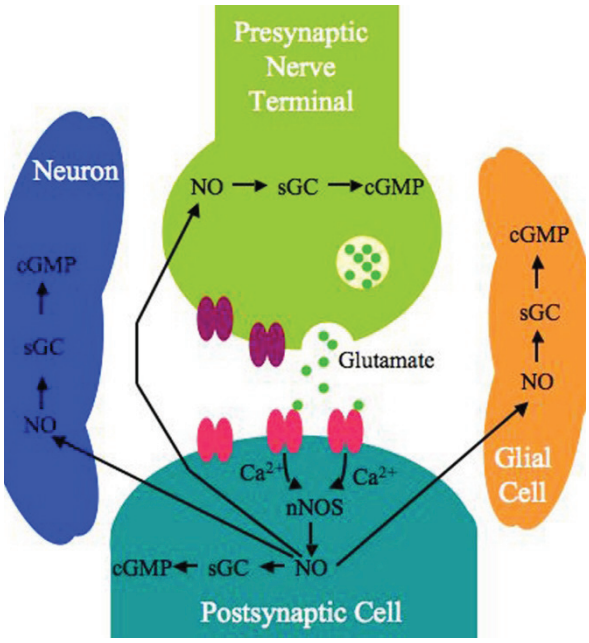

Figure 1.5: A drawing of a synapse that produces NO and leads to many cellular responses.

Nitric oxide was determined to diffuse from the post-synaptic cell and influence the pre-synaptic nerve and nearby glial and neuronal cells.[52] Nitric oxide also has been confirmed to be produced in pre-synaptic and post-synaptic cells.[53] This process is summarized in a cartoon in Figure 1.5.

1.5 Nitric Oxide Hypothesized Role in Cell Migration

Cellular migration is essential in the development of the nervous system and the anatomy of the brain in embryos. These processes require precise movement of cells where neurons can travel millimeters or centimeters. Nitric oxide is implicated is in neuronal development studies have found strong evidence.[54] Gibbs et al. demonstrated through *in vitro* studies that NO and cGMP may be involved in the stabilization of retinal growth cone, which provides the foundation for the development of the visual system.[55] Using the olfactory system as a model to study the potential of NO for chemical signaling, Roskams et al. were able to show that NO had a prominent role in forming connections in developing and regenerating olfactory neurons.[56] Another set of *in vitro* studies performed by Kalb et al. support the role of NO in the development of motor neurons in rat models.[57]

1.6 Classes of NO Donors

Nitric oxide donors are compounds that store NO in air stable form. Over 15 types of NO donor classes exist, allowing researchers to select an NO donor that is appropriate to their specific experimental system. These donor classes have been developed to release NO based on unique chemistries. As such, specific NO donors can be selected based on the timescales required for the application.

Below are six common NO donor classes and representative compound from each of these classes (Figure 1.6).

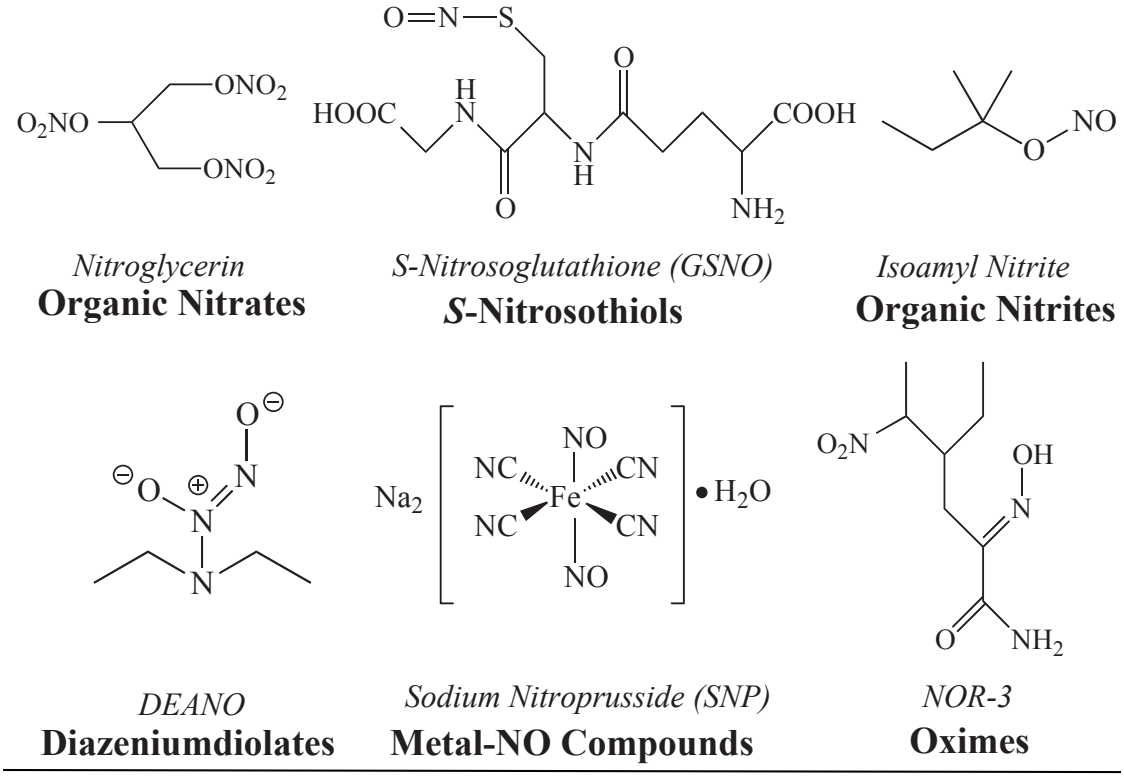

Figure 1.6: Above are 6 molecules each from different classes of NO donors: organic nitrates, *S*-nitrosothiols, organic nitrites, diazeniumdiolates, metal-NO compounds and oximes.

These featured NO donors are documented in numerous studies looking at the role of NO as it applies to the collective understanding of physiological processes.[58, 59, 60] In a study looking at understanding NO role in development of nerve networks, Wagenen et al. demonstrated that the uses of DEA/NO and SNP stimulated the increased the elongation of filopodial, cellular branches coming from a central growth cone produced by promoting nerve growth in B5 neurons.[54] NOR-3 was used to understand NO's influence on apoptosis in human colon cells by varying the NO donor concentration and relating apoptosis to an artifact NO through hormone signaling.[61] Nitric oxide donor, specifically

SNP and sodium nitrite, were used to show that NO may contribute to the formation of synapses and stimulate neurite out growth.[62] Nitroglycerin was used in a study interested in understanding NO effect on tumor development in mice models and they found that NO release from the NO donor caused a decrease in the growth of tumors through an enhancement in cell apoptosis.[63] Another study investigated the effect of NO to either protect or promote tissue from hydrogen peroxide mediated cytotoxic effects using three of the NO donors, DEA/NO, SNP and GSNO.[64] Wink et al. found that DEA/NO and GSNO protected the fibroblasts from the cytotoxic effects of hydrogen peroxide; however, SNP did not protect the cells. An important finding from this work was that the concentration of NO could be correlated to the fibroblasts growth.

These NO donors store and release NO through various mechanisms and an understanding of these basic mechanisms is important when choosing the ideal NO donor for any application. For example, organic nitrates release NO by a three-electron reduction, which can be performed via either an enzymatic or non-enzymatic pathway.[59] Organic nitrites generate NO by a one-electron reduction by hydrolyzing nitrite that then is reduced to NO. Metal-NO compound release NO by enzymatic reduction or one electron reduction by thiols, hemoproteins. Metal-NO donors are photosensitive and need to be protected to keep stable.[58] *S*-nitrosothiols can decompose by thermal, photochemical and copper-mediated decomposition.[65] Oximes release NO though a proposed radical decomposition at basic pH. Diazeniumdiolates, on the other hand, decompose by an acid-catalysed decomposition, and the NO release rate is very dependent on pH and temperature.[66]

Diazeniumdiolates have been used extensively because they are bench-top, air stable NO donors and yield reproducible NO release profiles at physiological pH with variable kinetic rates. The kinetic variability of these diazeniumdiolates was demonstrated by Hrabie et al. where they showed that NO release varied with temperature and chemical structure of the donor.[66] Davies et al. showed that the kinetic release of NO from diazeniumdiolates was also pH dependent.[67] Diazeniumdiolates have also been used to understand NO's role in biology by mixing into or covalently attaching the moiety to polymeric materials. In one example, a small molecule NO donor was used in a coating to improve the function of vascular grafts.[68,69] In an another study looking at killing tumors resistant to other chemotheraphy treatments, Liu et al. demonstrated that diazeniumdiolates could be a promising treatment.[70] This treatment was successful by providing selective release of NO by reacting with a *S*-transferases in the tumor cells to overcome the cells resistances to arsenic and cisplatin.[70] In a similar manner, because diazeniumdiolates have well-established decomposition kinetics, two diazeniumdiolates with different half-lives will be used in this work, MAHMA/NO and DETA/NO. There structures and half-lives are shown in Figure 1.7.

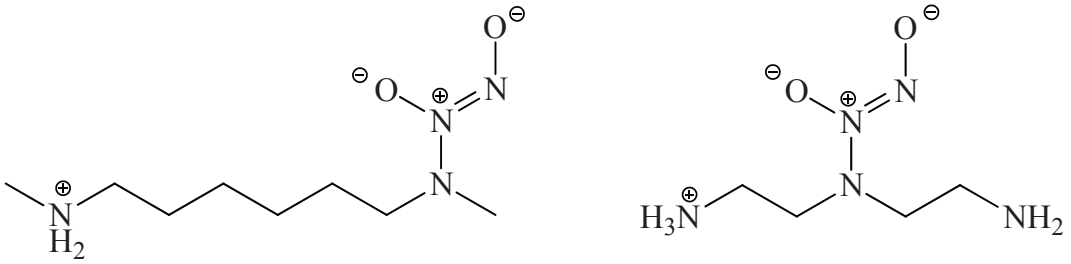

Half-life – 60 s
MAHMA/NO

Half-life – 20 h
DETA/NO

Figure 1.7: The chemical structures of MAHMA/NO (left) and DETA/NO (right) are shown above. Both compounds are diazeniumdiolates, a class of NO donors.

1.7 Nitric Oxide Detection Methods

With NO being involved in many biological processes, a need exists for quantitative detection methods that can be used to evaluate and understand the role of NO. There are two environments that NO measurements are needed: *in vivo* or *in vitro*. *In vivo* measurements look at quantifying the amount of endogenous NO that is produced in different regions of a living organism in order to better understand how NO influences cellular behavior within that model. In contrast, *in vitro* measurements attempt to recreate *in vivo* conditions with cell or tissue models to study NO's effect in a controlled and artificial environment.

Several detection methods and assays have been developed to assess NO concentrations directly and indirectly through decomposition products or secondary products (nitrosyl, nitrite, cGMP). Direct detection of NO is important to ensure NO is indeed detected and not a secondary product N_xO_y. In many cases, these direct methods are used when studying and quantifying NO in more fundamental systems. In more complex systems such as cell and tissue models, many still quantify NO using assays that monitor byproducts to estimate the amount of NO in the system.

Electrochemical Detection

The most commonly employed direct NO measurement technique is electrochemical detection. One of the major reasons for this is that electrochemical detection has extremely low detection limits. For example, in 1990, Shibuki and coworkers, developed an electrochemical microprobe, 150- 200 μm in diameter that was inserted into a 400 μm cerebellar rat slice followed by electrical stimulation of the tissue resulting in an observed NO concentration ranging between 8 and 58 nM.[71] A later study

using similar electrochemical probes on 400 μm auditory cortex brain slices that were electrically stimulated found NO release in 380±14 pM.[72] Building off the work done previously by the Shibuki group, a platinized carbon fiber microelectrode with a 5-7 μm diameter was used to establish a maximum local concentration of NO of 1.8±0.2 μM at 10 to 30 μm depth in rat cerebellar tissue slice after a 5 min stimulation in a 100 μM bath of N-methyl D-aspartate (NMDA).[73] From these various studies using electrochemical detection, a dynamic range of 1800 to 0.38 nM has been established for the expected range for physiological release of NO in brain tissue.[74]

Since electrochemical detection of NO is more common, many different approaches exist to electrochemically detect NO and the electrode design. These different approaches come with certain inherent strengths and weaknesses. The basic principle behind electrochemical detection is that a negative or positive potential is applied to the electrode and then the electrode reduces or oxidizes an electrochemically active species, which produces a current that is proportional to that species concentration. The most common electrochemical technique for measuring NO is amperometry, which allows users to quickly collect low current outputs at a fixed potential. The fast response time makes this type of electrochemical detection ideal for biological systems. Other electrochemical detection methods have been used to monitor NO; however, for the purpose of this overview, only amperometric systems will be discussed.[8] Since there are two types of potentials used in amperometric systems, there are two strategies for measuring NO directly at an electrode.

Reduction of NO at an electrode can occur via a 2 electron, shown in Figure 1.8, at negative potential ranging from -0.5 to -1.4 volts compared to a Ag/AgCl reference electrode.[75]

$$2\,NO + 2\,e^- \rightarrow N_2O_2^{2-}$$

Figure 1.8: An expression for the 2 electron reduction of NO at negative potential in electro-reduction detection systems for NO.

Electrochemical reduction of NO is a less frequently used approach for detecting NO because these systems tend to have lower sensitivity, slower scan rates, oxygen interferences, and difficulty in detecting at physiological pH.[76] A major challenge with detection of NO at negative potentials is the influence of oxygen on the signal because the standard reduction potential for oxygen is -1.229 V with respect to the standard hydrogen electrode.[77] Thus, to monitor NO effectively, the oxygen interference must be successfully subtracted out to achieve an accurate NO detection reading.

Because of the challenges associated with reductive electrochemical detection of NO, is another approach to detect NO is through the oxidation of NO, accomplished in 3 steps at positive potential as shown in Figure 1.9.

$$NO \rightarrow NO^+ + e^-$$
$$NO^+ + OH^- \rightarrow HNO_2$$
$$HNO_2 + H_2O \rightarrow NO_3^- + 2\,e^- + 3\,H^+$$

Figure 1.9: An expression for the 3 electron oxidation of NO at positive potential in electro-oxidation detection systems for NO.

When using positive potential to measure NO, concern exists that nitrite is produced in the final step may of the oxidation and may give a false high signal. As such, researchers need to be careful when selecting a potential, where only NO is detected. This is

especially the case in biological applications where the potential for other sources of nitrite to be present or formed through various side-reactions is real.[78] This is only one of the limitations that need to be overcome to improve electrochemical detection of NO as there are several other species that can interfere with the NO signal. Depending on the electrochemical system used to monitor NO several factors are involved with limiting the influence of interferences: sensor type, active potential, type of selective membrane and biological environment.[79] Several common species that interfere with the electrochemical detection of NO are highlighted in Table 1.2.

Table 1.2: Common Biological Interferences in Electrochemical Detection of NO[79]

Name	Physiological Concentration
Nitrite	< 20 μM
Ascorbic Acid	34 - 144 μM
Uric Acid	150 - 470 μM
Acetaminophen	66 - 199 μM
Carbon Monoxide	0.5 - 1.5 μM
Dopamine	< 2.0 nM
Norepinephrine	0.35 - 2.96 nM
Serotonin	0.28 - 1.14 μM
3,4-dihydroxyphenylacetic acid (DOPAC)	5.88 - 23.10 nM
5-hydroxyindole-3-acid (5-HIAA)	18.31 - 695.91 nM

In order to improve the overall selectivity of electrochemical detection and minimize some of these interferences, one common strategy employed is to coat the electrode surface with a selective membrane, like nafion. Nafion is used to minimize NO conversion into byproducts (i.e. nitrite) from being produced by stabilizing the forming NO^+ species within the membrane. Nafion can selectively repealing anionic interfering

species making it advantageous for use to minimize nitrite, but cannot minimize cationic interferences such as dopamine.

Electron Paramagnetic Resonance

Electron paramagnetic resonance (EPR) is another direct detection method that has been successfully used to monitor NO in biological systems. This technique has proven useful in measuring NO directly in living tissues and organs.[80] This technique is frequently used to understand the complex binding phenomena between NO and the heme group in hemoglobin.[81]

This technique is used to monitor any paramagnetic radical species, which has unpaired electrons that can be promoted to higher energy levels by a required amount of microwave frequency.[82] The basic idea behind EPR detection is that the unpaired π orbital electron is excited by a microwave frequency that excites the electron into higher energy levels and as that electron relaxes a unique signal is emitted. However, this simplistic explanation of EPR is not how NO is monitored via EPR because the electron that is excited in NO radicals has a relaxation time which is much too fast to detect. NO is studied using a technique called spin trapping. Spin trapping allows for the complete conversion of NO into a more stable radical that allows the characteristic EPR signal to be recorded (Figure 1.10).

$$R^{*} + ST \rightarrow NO - SA^{*}$$

Figure 1.10: An expression explaining how NO or any radical of interest (R*) is trapped by reacting with a species (ST) that traps the radical quickly to create a more stable radical trap addict (R*-SA).

Spin trapping, in principal, seems straightforward; however, in practice, it has been far more challenging to implement since spin trap molecules are not radical species, thus not detectable via EPR. There are two prominent spin trap molecules used extensively in the literature to look at NO by EPR detection. These molecules are hemoglobin, an excellent endogenous spin trap and iron-dithiocarbamates, an exogenous spin trap used in many studies. The EPR signal is generated from the relaxation on an excited electron in that moment the energy difference between the two possible signs ($M_s \pm ½$) is equal to microwave energy.[83] EPR signal gives researchers specific information about interactions of unpaired electrons. Hyperfine and superfine spectral features can be used to confirm spectra origin from electron spin coupling as in nuclear magnetic resonance.[84]

There are some inherent advantages for using EPR *in vivo* systems since tissue and biological systems often contain a spin trapping agent, such as hemoglobin (Hb). An added benefit to NO detection with Hb, is that EPR selectivity favors Hb-NO (paramagnetic) over Hb-O_2 and Hb-CO_2 (diamagnetic). The paramagnetic specificity has eliminated inflation in signal from possible sources of interferences in nitrite and nitrate. The overall sensitivity of EPR suffers because of the broad range of magnetic field strength used to initiate an EPR signal; however, to some degree this can be compensated by performing EPR studies at low temperature.[84] Sensitivity may interfere with collecting measurements that must be performed at physiological conditions. Using iron-dithiocarbamate spin trapping agent, EPR has a detection limit of ~6 pmol for NO.[85]

The underlying theory behind EPR detection of NO is based on quantum mechanics. Therefore the use of conventional and advanced EPR is very complex and data analysis can be challenging especially when identifying spin interaction represented

by the appearance of hyperfine and superfine structure on spectra. This detection system has allowed researcher to learn novel insights to deepen the collective understanding of NO's role in biology with the ability to make qualitative and quantitative measurements of NO. This system is not well suited for developing a straight forward and streamlined measurement method for detecting NO release from NO donor in cellular media buffered by carbon dioxide.

Chemiluminescence

The final direct detection technique for NO is chemiluminescence. Chemiluminescence has been used to produce reliable NO release profile for a variety of NO donor and NO releasing polymeric materials.[86,87,68,88] The ozone chemiluminescence method is a sensitive technique that allows for detection of NO in real time and total recovery of NO that is introduced to the system. This technique works by reacting gaseous NO with ozone, formed in the instrument, to create an excited state nitrogen dioxide (NO_2^*) species that decays to the ground state emitting a photon (Figure 1.11).[89]

$$NO + O_3 \rightarrow NO_2^* + O_2$$
$$NO_2^* \rightarrow NO_2 + h\nu$$

Figure 1.11: An expression explaining how NO is detected using chemiluminescence.

The amount of light that is generated can then be directly related to the concentration of NO by a calibration constant determined by the reduction of nitrite to NO by hydrosulfuric acid and confirmed using any NO donor. Detection of any light is directly tied to the relase of NO eliminating the potential for interference. The detection limits for ozone chemiluminescence detection system is reported to be ~10 pmol, making this an excellent technique to look at physiological levels of NO.[90]

Although chemiluminescence is an excellent technique to monitor NO, the technique requires that the system be deoxygenated, making *in vivo* studies challenging. However, this system is very beneficial for the development of a bench-top, real-time measurement method to analyze NO release from commonly used NO donor in conditions that mimic those used in *in vitro* studies to gauge NO's cellular influence.

NO detection in Cell and Tissue media

Literature precedent for a bench-top cell media-based detection system for NO, nitrite and nitrate was published by Ridnour et al., where they used an indirect spectroscopic assay to approximate the amount of NO, nitrite and nitrate.[91] Based on shifting the pH, they claimed to resolve the approximate the concentration of NO, nitrite and nitrate in 10% cell media buffered by 90% PBS (pH 7.40).[91] This experiment is a great example of how many cell and tissue models are analyzed for apparent NO. However, Ridnour's system lacks three essential requirements for measuring NO in tissue media. The first is direct detection of NO that eliminates false positive signals from N_xO_y species. The other important features lacking in this method include the ability to measure NO release in real time and to use full strength tissue media buffered by CO_2.

There have been reports of electrochemical detection of NO in tissue media.[92] However, many of these *in vitro* NO detection experiments employ 4-(2-hydroxyethyl)-1-piperazineethanesulfonic acid (HEPES) or tris(hydroxymethyl)aminomethane (TRIS) buffer to buffer the tissue media at pH 7.40 instead of CO_2.

1.8 Summary

Nitric oxide has a significant role in biological system. Researchers now understand how NO is produced *in vivo* and that most of the cellular responses are regulated through the secondary signaling molecule, cGMP. In order to begin to use this knowledge to combat diseases and disorders that can be linked to NO deficiencies, additional analytical detection methods are needed to be able to accurately monitor NO concentrations. As previously discussed, several NO measurement methods exist, but limited methods are available that allow for detection under conditions commonly used in *in vitro* cell and tissue model studies, specifically where the medias is buffered by carbon dioxide.

In this thesis, I will present a measurement method developed to measure physiological levels of NO from NO donors in a bench-top system equipped to mimic conditions used in cell and tissue studies. This method will aim to demonstrate 1) detection of NO from a 10^{-7} M NO donor (MAHMA/NO) in phosphate buffered saline (PBS) and 2) detection of NO release from NO donors (MAHMA/NO and DETA/NO) in tissue media buffered by CO_2. The first aim focuses on modifying the current chemiluminescence methodology for NO donor concentrations from 10^{-4} M to 10^{-7} M enabling this measurement method to monitor a wider range of NO donor concentrations. The significant of this method development will be to allow researcher to measure accurate NO releases profile for a wide range of NO donor concentration that could be used in therapeutic applications. The second aim focuses on developing an accurate NO release measurement method that will allow NO donors to be studied in buffered tissue media. Tissue media buffered by CO_2 is used frequently in many biologically relevant

experiments looking at the effect of NO. However, current methods typically use PBS since the buffer can be set to physiological conditions (37 °C, pH 7.40). This buffering system is not used in cell and tissue model experiments because it does not contain the necessary nutrients required to artificially sustain the cells. Tissue media, which contains over 25 essential elements, is typically buffered with CO_2 gas to maintain the pH at 7.40 by employing a carbonic acid and bicarbonate buffering system.

Figure 1.12 shows a flow chart, which outlines the design of separate experiments to be able to create a complete and functioning methodology using a step-wise approach.

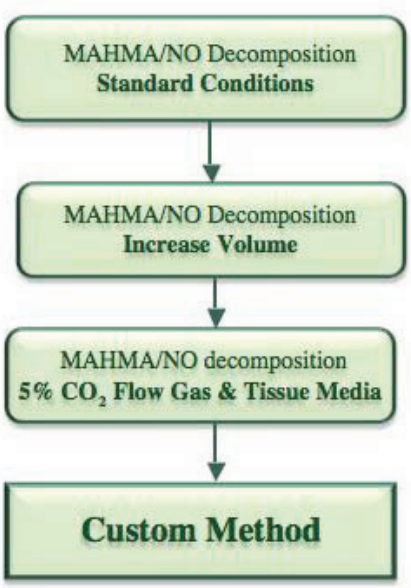

Figure 1.12: Flow chart showing the experimental development of custom method based on MAHMA/NO decomposition.

The first step is to measure NO release from the decomposition of NO donor and calculate the donor decomposition half-lives. Three main factors will be used to establish the measurement method effective: accurate donor release kinetics, total NO recovery and ability to maintain pH 7.4 and 37 °C. The rationale for this approach was to begin in a simple model system and show that the decomposition of MAHMA/NO can be

monitored by NO release. Once the measurement method is functioning at the 2 mL volume, slight incremental changes to the volume can be made to the method. As the volume increases the total NO recovery and accurate donor decomposition half-lives was achieved by adjusting the gas regulation. The increase in buffer volume will allow for more dilute NO donor solutions to be monitored with this chemiluminescence measurement method. Once the method could reliably achieve complete NO recovery and accurate donor decomposition half-lives the method could be expanded from a simplistic buffer system to tissue media buffered by 5% CO_2. This measurement method can be used to measure NO release profile from NO donor at lower concentrations and under conditions that more closely mirror those of *in vitro* experiments.

1.9 References

1. Sprigge, J. S., Sir Humphry Davy; his researches in respiratory physiology and his debt to Antoine Lavoisier. *Anaesthesia* **2002**, 357-364.
2. Heywood, J. B., *Internal Combustion Engine Fundamentals*. McGraw Hill: New York, 1988; p 20.
3. Donahue, N. M., The reaction that wouldn't quit. *Nature Chemistry* **2011,** *3*, 98-99.
4. Ignarro, L. J.; Byrns, R. E.; Buga, G. M.; Wood, K. S., Endothelium-derived relaxing factor from pulmonary artery and vein possesses pharmacologic and chemical properties identical to those of nitric oxide radicals. *Circulation Research* **1987,** *61*, 866-879.
5. Palmer, R. M. J.; Ferrige, A. G.; Moncada, S., Nitric oxide release account for the biological activity of endothelium-derived relaxing factor. *Nature* **1987,** *327*, 524-526.
6. Ignarro, L. J.; Buga, G. M.; Wood, K. S.; Byrns, R. E.; Chaudhuri, G., Endothelium-derived relaxing factor produced and released from artery and vein is nitric oxide. *Proceeding of the National Academy of Science* **1987,** *84*, 9265-9269.
7. Bogdan, C., Nitric Oxide and the immune response. *Nature Review Immuniology* **2001,** *2* (10), 907-916.
8. Davies, I. R.; Zhang, X., Nitric Oxide Selective Electrodes. In *Methods in Enzymology*, 2008; Vol. 436, pp 63-95.
9. Saavedra, J. E.; Keefer, L. K., Nitrogen-Based Diazeniumdiolates: Versatile Nitric Oxide-Releasing Compounds in Biomedical Research and Potential Clinical Applications. *Journal of Chemical Education* **2002,** *79* (12), 1427-1434.
10. Ignarro, L. J., Nitric Oxide as a Unique signaling molecule in the Vascular System: A Historical Overview. *Journal of Physiology and Pharmacology* **2002,** *53* (4), 503-514.
11. Katsuki, S.; Arnold, W.; Mittal, C.; Murad, F., Stimulation of guanylate cyclase by sodium nitroprusside, nitroglycerin and nitric oxide in various tissue preparations and comparison to the effects of sodium azide and hydroxylamine. *Journal of Cyclic Nucleotide Research* **1977,** *3*, 23-5.
12. Marsh, N.; Marsh, A., A Short History of Nitroglycerin and Nitric Oxide in Pharmacology and Physiology. *Clinical and Experimental Pharmacology and Physiology* **2000,** *27*, 313-319.
13. Mellion, B. T.; Ignarro, L. J.; Ohlstein, E. H.; Pontecorvo, E. G.; Hyman, A. L.; Kadowitz, P. J., Evidence for the inhibitory role of guanosine3', 5'-monophosphate in ADP-induced human platelet aggregation in the presence of nitric oxide and related vasodilators. *Blood* **1981,** *57* (3), 946-955.
14. Furlong, B.; Henderson, A. H.; Lewis, M. J.; Smith, J. A., Endothelium-derived relaxing factor inhibits in vitro platelet aggregation. *British Journal of Pharmacology* **1987,** *90*, 687-692.
15. Traylor, T. G.; Sharma, V. S., Why NO? *Biochemistry* **1991,** *31* (11), 2847-2848.
16. Rees, D. D.; Palmer, R. M. J.; Moncada, S., Role of endothelium-derived nitric oxide in the regulation of blood pressure. *Proceedings of the National Academy of Science* **1989,** *86*, 3375-3378.

17. Gardiner, S. M.; Compton, A. M.; Bennett, T.; Palmer, R. M.; Moncada, S., Control of regional blood flow by endothelium-derived nitric oxide. *Hypertension* **1990,** *15*, 486-492.
18. Dupuy, P. M.; Shore, S. A.; Drazen, J. M.; Frostell, C.; Hill, A. W.; Zapol, W. M., Bronchodilator Action of Inhaled Nitric Oxide in Guinea Pigs. *Inhaled Nitric Oxide Bronchodilation* **1992,** *90*, 421-428.
19. Belvisi, M. G.; Stretton, C. D.; Yacoub, M.; Barnes, P. J., Nitric oxide is the endogenous neurotransmitter of bronchodilator nerves in humans. *European Journal of Pharmacology* **1992,** *210*, 221-222.
20. Gustafsson, L. E.; Leone, A. M.; Persson, M. G.; Wiklund, N. P.; Moncada, S., Endogenous nitric oxide source in the exhaled air of rabbits, guinea pigs, and humans. *Biochemical and Biophysical Research Communications* **1991,** *181*, 852-857.
21. Kharitonov, S. A.; Yates, D.; Barnes, P. J.; Logan-Sinclair, R.; Shinebourne, E. A., Increased nitric oxide in exhaled air of asthmatic patients. *The Lancet* **1994,** *343* (8890), 133-135.
22. Belvisi, M. G.; Stretton, C. D.; Yacoub, M.; Barnes, P. J., Nitric oxide is the endogenous neurotransmitter of bronchodilator nerves in humans. *European Journal of Pharmacology* **1991,** *210*, 221-222.
23. Moilanen, E.; Vapaatalo, H., Nitric Oxide in Inflammation and Immune Response. *Annals of Medicine* **1995,** *27* (3), 359-367.
24. Tripathi, P., Nitric Oxide and Immune Response. *Indian Journal of Biochemistry & Biophysics* **2007,** *44*, 310-319.
25. MacMicking, J.; Xie, Q.-w.; Nathan, C., Nitric Oxide and Macrophage Function. *Annual Review of Immunology* **1997,** *15*, 323-350.
26. Fang, F. C., Mechanisms of Nitric Oxide-related Antimicrobial Activity. *Journal of clinical investigation* **1997,** *99* (12), 2818-2825.
27. Calabrese, V.; Mancuso, C.; Calvani, M.; Rizzarelli, E.; Butterfield, D. A.; Stella, A. M. G., Nitric oxide in the central nervous system: neuroprotection versus neurotoxicity. *Nature Neuroscience* **2007,** *8*, 766-775.
28. Meller, S. T.; Gebhart, G. F., Nitric Oxide (NO) and nociceptive processing in the spinal cord. **1993,** *52*, 127-136.
29. Holthusen, H.; Arndt, J. O., Nitric Oxide evokes pain in humans on intracutaneous injections. *Neuroscience Letters* **1994,** *165*, 71-74.
30. Zhang, X.; Verge, V.; Wiesenfeld-Hallin, Z.; Ju, G.; Bredt, D.; Synder, S.; Hokfelt, T., Nitric Oxide synthase-like immunoreactivity in lumbar dorsal root ganglia and spinal cord of rat and monkey and effect of peripheral axotomy. *Journal of Comparative Neurology* **1993,** *335* (4), 563-575.
31. Aley, K. O.; McCarter, G.; Levine, J. D., Nitric Oxide Signaling in Pain and Nociceptor Sensitization in the Rat. *Journal of Neuroscience* **1998,** *18* (17), 7008-7014.
32. Gautier-Sauvigne, S.; Colas, D.; Parmantier, P.; Clement, P.; Gharib, A.; Sarda, N.; Cespuglio, R., Nitric oxide and sleep. *Sleep Medicine Reviews* **2005**, 101-113.
33. Takahashi, T., Pathophysiological significance of nueronal nitric oxide synthase in the gastrointestinal tract. *Journal of Gastroenterol* **2003,** *38*, 421-430.
34. Vozzo, R.; Wittert, G. A.; Horowitz, M.; Morley, J. E.; Chapman, I. M., Effect of nitric oxide synthase inhibitors on short-term appetite and food intake in humans.

American Journal of Physiology - Regulatory, Integrative and Comparative Physiology **1999,** *276*, R1562-R1568.
35. Garthwaite, J.; Charles, S. L.; Chess-Williams, R., Endothelium-derived relaxing factor release on the activation of NDMA receptors suggests role as intercellular message in the brain. *Nature* **1988,** *336*, 385-388.
36. Mayer, B.; Schmidt, K.; Humbret, P.; Bohme, E., Biosynthesis of endothelium-derived relaxing factor: a cytosolic enzyme in porcine aortic endothelium cells Ca^{2+}-dependently converts L-arginine into an activator of soluble guanylyl cyclase. *Biochemical and Biophysical Research Communications* **1989,** *184* (2), 678-685.
37. Dawson, T. M.; Synder, S. H., Gases as Biological Messengers: Nitric Oxide and Carbon Monoxide in the Brain. *The Journal of Neuroscience* **1994,** *14* (9), 5147-5159.
38. Guix, F. X.; Uribesalgo, I.; Coma, M.; Munoz, F. J., The physiology and the pathophysiology of nitric oxide in the brain *Progress in Neurobiology* **2005,** *76*, 126-152.
39. Bredt, D. S.; Hwang, P. M.; Snyder, S. H., Localization of nitric oxide synthase indicating a nueral role of nitric oxide. *Nature* **1990,** *347*, 768-770.
40. Griffith, O. W.; Stuehr, D. J., Nitric Oxide Synthases: Properties and Catalytic Mechanism. *Annual Review of Physiology* **1995,** *57*, 707-736.
41. Hevel, J. M.; White, K. A.; Marletta, M. A., Purification of the Inducible Murine Macrophage Nitric Oxide Synthase. *Journal of Biological Chemistry* **1991,** *266* (34), 22789-22791.
42. Pollock, J. S.; Forstermann, U.; Mitchell, J. A.; Warner, T. D.; Schmidt, H. H. H. W.; Nakane, M.; Murad, F., Purification and characterization of particulate endothelium-derived relaxing factor synthase from cultured and native bovine aortic endothelial cells. *Proceeding of the National Academy of Science* **1991,** *88*, 10480-10484.
43. Dimmeler, S.; Fleming, I.; Fisslthaler, B.; Hermann, C.; Busse, R.; Zeiher, A. M., Activation of nitric oxide synthase in endothelial cells by Akt-dependent phosphorylation. *Nature* **1999,** *399*, 601-605.
44. Zhou, L.; Zhu, D.-Y., Nueronal nitric oxide synthase: Structure, subcellular localization, regulation and clinical implications. *Nitric Oxide* **2009,** *20*, 223-230.
45. Mohammed, N. A.; El-Aleem, S. A.; Appleton, I.; Maklouf, M. M.; Said, M.; McMahon, R. F. T., Expression of nitric oxide synthase isoforms in human liver cirrhosis. *Journal of Pathology* **2003,** *200* (5), 647-655.
46. Murad, F., Discovery of Somoe of the Biologicak Effects of Nitric Oxide and Its Role in Cell Signaling (Nobel Lecture). *Angewandte Chemie International Edition* **1999,** *38*, 1856-1868.
47. Arnold, W. P.; Mittal, C. K.; Katsuki, S.; Murad, F., Nitric oxide activates guanylate cyclase and increase guanosine 3':5'-cyclic monophosphate levels in various tissue preparations. *Proceeding of the National Academy of Science* **1977,** *74* (8), 3203-3207.
48. Denninger, J. W.; Marletta, M. A., Guanylate cyclase and the NO/cGMP signaling pathway. *Biochimica et Biophysica Acta* **1999**, 334-350.
49. Ziche, M.; Morbidelli, L., Nitric Oxide and Angiogenesis. *Journal of Neuro-Oncology* **2000,** *50*, 139-148.
50. Valenstein, E. S., The Discovery of Chemical Neurotransmitters. *Brain and Cognition* **2002,** *49*, 73-95.

51. Deutch, A. Y.; Roth, R. H., Pharmacology and Biochemistry of Synaptic Transmission:Classic Transmitters. In *From molecules to networks: An introduction to Cellular and Molecular Neuroscience*, Byrne, J. H.; Roberts, J. L., Eds. Elsevier: San Diego, 2004; pp 245-278.
52. Garthwaite, J., Glutamate, nitric oxide and cell-cell signaling in the nervous system. *Trends in Neuroscience* **1991,** *14* (12), 60-67.
53. Garthwaite, J., Concepts of neural nitric oxide-mediated transmission. *European Journal of Nueroscience* **2008,** *27*, 2783-2802.
54. Wagenen, S. V.; Rehder, V., Regulation of Neuronal Growth Cone Filopodia by Nitric Oxide. *Journal of Neurobiology* **1999,** *39* (2), 168-185.
55. Gibbs, S. M.; Truman, J. W., Nitric Oxide and cyclic GMP regulates retinal patterning in the optic lobe of *Drosphila*. *Neuron* **1998,** *20*, 83-93.
56. Roskams, A. J.; Bredt, D. S.; Dawson, T. M.; Ronnett, G. V., Nitric Oxides Mediates the Formation of synaptic connections in Developing annnd regenerating olfactory receptor neurons. *Neuron* **1994,** *13*, 289-299.
57. Kalb, R. G.; Agostini, J., Molecular evidence for nitric oxide-mediated motor neurons development. *Neuroscience* **1993,** *57* (1), 1-8.
58. Feelisch, M.; Stamler, J. S., Donors of Nitrogen Oxides. In *Methods in Nitric Oxide Research*, Feelisch, M.; Stamler, J. S., Eds. John Wiley & Sons: New York, 1996; pp 71-115.
59. Wang, P. G.; Xian, M.; Tang, X.; Wu, X.; Wen, Z.; Cai, T.; Janczuk, A. J., Nitric Oxide Donors: Chemical Activities and Biological Applications. *Chemical Reviews* **2002,** *102* (4), 1091-1134.
60. Yamamoto, T.; Bing, R. J., Nitric Oxide Donors. *Proceedings of the Society for Experimental Biology and Medicine* **2000,** *225*, 200-206.
61. Marino, M.; Galluzo, P.; Leone, S.; Acconcia, F.; Ascenzi, P., Nitric oxide impairs the 17-estradiol-induced apoptosis in human colon adenocarcinoma cells. *Endocrine-Related Cancer* **2006,** *13*, 559-569.
62. Hindley, S.; Juurlink, B. H. J.; Gysbers, J. W.; Middlemiss, P. J.; Herman, M. A. R.; Rathbone, M. P., Nitric Oxide Donor Enhance Neurotrophin-Induced Outgrowth through a cGMP-Dependent Mechanism. *Journal of Neuroscience Research* **1997,** *47*, 427-439.
63. Trikha, P.; Sharma, N.; Athar, M., Nitriglycerin: a NO donor inhibits TPA-mediated tumor promotion in murine skin. *Carcinogensis* **2001,** *22* (8), 1207-1211.
64. Wink, D. A.; Cook, J. A.; Pacelli, R.; DeGraff, W.; Gamson, J.; Liebmann, J.; Krishna, M. C.; Mitchell, J. B., The effect of various nitric oxide-donor agents on hydrogen peroxide-mediated toxicity: a direct correlation between nitric oxide formation and protection. *Archives of Biochemistry and Biophysics* **1996,** *331* (2), 241-248.
65. Al-Sa'Doni, H.; Ferro, A., S-Nitrosothiols: a class of nitric oxide-donor drugs. *Clinical Science* **2000,** *98*, 507-520.
66. Hrabie, J. A.; Klose, J. R.; Wink, D. A.; Keefer, L. K., New Nitric Oxide-Releasing Zwitterions Derived from Polyamines. *Journal of Organic Chemistry* **1993,** *58* (6), 1472-1476.
67. Davies, K. M.; Wink, D. A.; Saavedra, J. E.; Keefer, L. K., Chemistry of the Diazeniumdiolates. 2. Kinetic and Mechanisms of Dissociation to Nitric Oxide in Aqueous Solution. *Journal of American Chemical Society* **2001,** *123* (23), 5473-5481.

68. Reynolds, M. M.; Hrabie, J. A.; Oh, B. K.; Politis, J. K.; Citro, M. L.; Keefer, L. K.; Meyerhoff, M. E., Nitric Oxide Releasing Polyurethane with Covalently Linked Diazeniumdiolated Secondary Amines. *Biomacromolecules* **2006,** *7* (3), 987-994.
69. Batchelor, M. M.; Reoma, S. L.; Fleser, P. S.; Nuthakki, V. K.; Callahan, R. E.; Shanley, C. J.; Politis, J. K.; Elmore, J.; Merz, S. I.; Meyerhoff, M. E., More Lipophillic Dialkyldiamine-Based Diazeniumdiolates: Synthesis, Characterization and Application in Preparing Thromboresistant Nitric Oxide Release Polymeric Coatings. *Journal of Medicinal Chemistry* **2003,** *46*, 5153-5161.
70. Liu, J.; Li, C.; Qu, W.; Lesile, E.; Bonifant, C. L.; Buzard, G. S.; Saavedra, J. E.; Keefer, L. K.; Waalkes, M. P., Nitric oxide prodrugs and mettallochemotherapeutics:JS-K and CB-3-100 enhance arsenic and cisplatin cytolethality by increasing cellular accumulation. *Molecular Cancer Therapeutics* **2004,** *3*, 709-714.
71. Shibuki, K., An electrochemical microprobe for detecting nitric oxide release in brain tissue. *Nueroscience Research* **1990,** *9*, 69-76.
72. Wakatsuki, H.; Gomi, H.; Kudoh, M.; Kimura, S.; Tasahashi, K.; Takeda, M.; Shibuki, K., Layer-specific NO dependence of long-term potentiation and biased NO release in layer V in the rat auditory cortex. *Journal of Physiology* **1998,** *513* (1), 71-81.
73. Amatore, C.; Arbault, S.; Bouret, Y.; Cauli, B.; Guille, M.; Rancillac, A.; Rossier, J., Nitric Oxide Release during Evoked Neuronal Activity in Cerebellum Slices: Detection with Platinized Carbon-Fiber Microelectrodes. *ChemPhysChem* **2006,** *7*, 181-187.
74. Hall, C. N.; Garthwaite, J., What is the real physiological NO concentration in vivo? *Nitric Oxide* **2009,** *21*, 92-103.
75. Ciszewski, A.; Milczarek, G., Electrode detection of nitric oxide using polymer modified electrode. *Talanta* **2003,** *61* (1), 11-26.
76. Bedioui, F.; Trevin, S.; Devnck, J., Chemically Modified Microelectrodes Designed for the Electrochemical Determination of Nitric Oxide in Biological System. *Electroanalysis* **1996,** *8* (12), 1085- 1091.
77. Vanysek, P., Electrochemical Series. In *CRC Handbook of Chemistry and Physics*, Lide, D. R., Ed. Taylor & Francis Group: New York, 2006; pp 8-20-8-29.
78. Lundberg, J. O.; Weitzburg, E.; Gladwin, M. T., The nitrate-nitrite-nitric oxide pathway in physiology and therapeutics. *Nature Reviews Drug Discovery* **2008,** *7* (2), 156-167.
79. Privett, B. J.; Shin, J. H.; Schoenfisch, M. H., Electrochemical nitric oxide sensor for physiological measurements. *Chemical Society Reviews* **2010,** *39*, 1925-1935.
80. Kuppusamy, P.; Shankar, R. A.; Roubaud, V. M.; Zweier, J. L., Whole body detection and imaging of nitric oxide generation in mice following cardiopulmonary arrest: Detectionof intrinsic nitrosoheme complexes. *Magnetic Resonance in Medicine* **2001,** *45* (4), 700-707.
81. Luchsinger, B. P.; Walter, E. D.; Lee, L. L.; Stamler, J. S.; Singel, D. J., EPR Studies of Chemical Dynamics of NO and Hemoglobin Interactions. *Biological Magnetic Resonance* **2009,** *28* (2), 419-438.
82. Archer, S., Measurement of nitric oxide in biological models. *The journal of the federation of american societies for experimental biology* **1993,** *7*, 349-360.

83. Kleschyov, A. L.; Wenzel, P.; Munzel, T., Electron paramagnetic resonance (EPR) spin trapping of biological nitric oxide. *Journal of Chromatography B* **2007,** *851*, 12-20.
84. Singel, D. J.; Lancaster, J. R., Electron Paramagnetic Resonance Spectroscopy and Nitric Oxide Biology. In *Methods in Nitric Oxide Research*, Feelisch, M.; Stamler, J. S., Eds. John Wiley & Sons: New York, 1996; pp 241-356.
85. Kleschyov, A. L.; Muller, B.; Keravis, T.; Stoeckel, M.-E.; Stoclet, J.-C., Adventitia-derived nitric oxide in rat aortas exposed to endotoxin:cell orgin and functional consequences. *American Journal of Physiology Heart and Circulatory Physiology* **2000,** *279*, H2743-H2751.
86. Reynolds, M. M.; Zhou, Z. Z.; Oh, B. K.; Meyerhoff, M. E., Bis-diazeniumdiolates of Dialkyldiamines: Enhanced Nitric Oxide Loading of Parent Diamines. *Organic Letters* **2005,** *7* (14), 2813-2816.
87. Frost, M. C.; Reynolds, M. M.; Meyerhoff, M. E., Polymers incorporating nitric oxide releasing/generating substances for improved biocompatibility of blood-contacting medical devices. *Biomaterials* **2005,** *26*, 1685-1693.
88. Damodaran, V. B.; Joslin, J. M.; Wold, K. A.; Reynolds, M. M., S-Nitrosated biodegradable polymers for biomedical applications: synthesis, characterization and impact of thiol structure on the physiocochemical properties. *Journal of Material Chemistry* **2012,** *22* (13), 5990-6001.
89. Bates, J. N., Nitric Oxide Measurements by Chemiluminescence Detection. *Nueroprotocols: A Companion to Methods in Nuerosciences* **1992,** *1* (2), 141-149.
90. Hetrick, E. M.; Schoenfisch, M. H., Analytical Chemistry of Nitric Oxide. *Annual Review of Analytical Chemistry* **2009,** *2*, 409-433.
91. Ridnour, L. A.; Sim, J. E.; Hayward, M. A.; Wink, D. A.; Martin, S. M.; Buettner, G. R.; Spitz, D. R., A Spectrophotometric Method for Direct Detection and Qauntification of Nitric Oxide, Nitrite and Nitrate in Cell Culture Media. *Analytical Biochemistry* **2000,** *281*, 223-229.
92. Keynes, R. G.; Griffiths, C.; Garthwaite, J., Superoxide-dependent consumption of nitric oxide in biological media may confound in vitro experiments. *Biochemical Journal* **2003,** *369*, 399-406.

2. METHOD DEVELOPMENT FOR MEASURING NO RELEASE FROM DILUTE NO DONOR SOLUTIONS

2.1 Introduction

Although the exact physiological concentration of nitric oxide (NO) for a variety of functions *in vivo* is still unknown, *in vivo* concentrations of 100 pM -1 μM have been reported.[1] Nitric oxide donors have been used in a variety of studies to better understand the role of NO in physiology.[2,3] In order to release NO within this physiological range, NO donors have been used at various concentrations to release NO that can influence cellular response *in vitro* studies.[2, 3,4] Several detections methods are commonly employed to accurately measure NO release from NO donor concentrations; in general, spectroscopic (10^{-3} M), electrochemical (10^{-6} M) and chemiluminescence (10^{-4} M) analysis have all been demonstrated. However, electrochemical methods have the ability to monitor NO release from a wider range of NO donor concentration than other techniques. Because NO donors are being explored as potential NO therapeutics and used *in vitro* studies to assess NO's influence in physiology, there is a need for the development of reliable analytical methods that allow researchers to measure accurate NO release profiles for a range of NO donor concentrations. These new methods will allow researchers to explore the full possibilities of using synthetic NO donors as potential therapeutic compounds to treat various illnesses and disorders.

In this chapter, I will demonstrate a significant improvement in the ability to measure NO release from a wider concentration range of the NO donor, Methylaminehexylmethylamine diazeniumdiolate (MAHMA/NO) through the

modification of a chemiluminescence based method to monitor NO release from 10^{-4} M to 10^{-7} M MAHMA/NO solutions.

2.2 Materials

Sulfuric acid (H_2SO_4, BDH), potassium iodide (KI, Fisher Scientific, 99.1%), sodium hydroxide (NaOH, Fisher Scientific, 99.8%), hydrochloric acid (HCl, BDH), phosphate buffered saline pressed tablets (PBS, EMD, 80-85% sodium chloride, 10-15% sodium phosphate [dibasic], 1-5% potassium chloride, 1-5% potassium phosphate [monobasic]) and sodium nitrite (Alfa Aesar, 99.999%) were purchased commercially and used as received. Methylaminehexylmethylamine (MAHMA, TCI America, 97%), 3 Å molecular sieves (Acros Organic, 8 to 12 mesh) and acetonitrile (CH_3CN, Sigma Aldrich, 99.5%) were purchased commercially and used to synthesis MAHMA/NO. MAHMA/NO was synthesized and purified in house following a detailed description described in section 2.3.1. All aqueous solutions were prepared using Millipore treated water (18.2 MΩ). Nitrogen (Ultra High Grade Purity) and oxygen (Medical grade) compressed gases for NO release measurements were purchased from Air Gas. The 45 ppm NO cylinder (Air Liquide, 98%) was used for daily calibration and ultra-high purity NO (Air Liquide, 99%) was used for NO donor synthesis.

2.3 Methods

2.3.1 Nitric Oxide Donor Synthesis

MAHMA/NO was prepared according to a previously published report by reacting the methylaminehexylmethylamine with NO at 80 psi in dry acetonitrile for 24 h.[5] Acetonitrile was dried over 3 Å molecular sieves prior to use. The solid white product was filtered off and washed with dry CH_3CN and dried under vacuum for approximately

three hours. The diazeniumdiolate was characterized for purity by UV spectroscopy at 250 nm and then stored in a -5 °C freezer until use.

2.3.2 Nitric Oxide Release Measurements

Nitric oxide measurements were performed using a Sievers Nitric Oxide Analyzer (NOA), model 280i. The instrumental sampling rate was set to 200 mL/min with a cell pressure ranging from 6.5 to 9.8 Torr and the oxygen supply pressure ranged from 4.2 to 6.9 psig.

Nitric Oxide Release 10^{-4} M MAHMA/NO Experiments in 2 mL

The initial protocol for the MAHMA/NO decomposition experiments were based on spectroscopic MAHMA/NO decomposition and NO release experiments previously published by Davies et al and Reynolds et al.[6,7] The NO donor stock solution for MAHMA/NO was prepared in 0.1 M NaOH and the concentration was confirmed by UV spectroscopy (250 nm). The bubbler gas was set to 16 mL/min rate and the flow gas was set at 184 mL/min, offsetting the 200 mL/min sampling rate to the detector. The NOA instrument's data collection interval was set to 1 s. The NOA instrument was calibrated daily with nitrogen (zero gas) and a 45 ppm NO standard. The sample cell was filled with 2 mL of PBS buffer at pH ~7.15 and the cell was sealed and hooked up to the bubble, flow and vacuum lines. The sample cell was degassed and then a baseline was collected. A calibrated syringe was used to inject 20 µl of the MAHMA/NO stock solution into the sample cell. Once the signal returned to a baseline reading, data collection was terminated and a final pH reading was recorded for the sample. This experiment was repeated 5 times in order to achieve reproducibly MAHMA/NO decomposition kinetics at this volume. Data analysis was performed in Excel and a

detailed protocol for how to process NO release data to elucidate MAHMA/NO half-lives is described below.

Nitric Oxide Release 10^{-4} M MAHMA/NO Experiments in 6, 8 and 10 mL

Nitric oxide release measurements were carried out similarly to the 2 mL 10^{-4} M MAHMA/NO experiments discussed previously, with variations to the injection volume and gas regulation for the increase in buffer volume in the 6, 8, and 10 mL case. In the 6 mL case, the bubbler gas was increased to 35 mL/min and then the flow gas was decreased to 173 mL/min to offset the 200 mL/min sampling rate of the vacuum with an injection volume of 60 µl. In the 8 mL case, the bubbler gas was set to 43 mL/min and the flow gas was set to 156 mL/min. An injection volume of 80 µl of the MAHMA/NO stock solution was used. In the 10 mL case using the custom 3-port NOA sample cell, the bubbler gas was set to 59 mL/min and the flow gas was set to 140 mL/min. An injection volume of 100 µl of the MAHMA/NO stock solution was used.

Nitric Oxide Release 10^{-7} M MAHMA/NO Experiments in 10 mL

Nitric oxide release measurements were performed similar to all other MAHMA/NO experiments discussed previously with a few modification to the injection volume and gas regulation settings. In order to perform the 4.4 x 10^{-7} M experiments using the 3-port NOA cell, a MAHMA/NO donor stock was determined to be 4.4 x 10^{-5} M by UV analysis and the bubble gas was set to 46 mL/min and the flow gas was set to 156 mL/min with an injection volume of 100 µl. A 100 µl of the MAHMA/NO stock solution was injected into the 10 mL PBS buffer.

Data Processing

MAHMA/NO decomposition data was processed using Excel. The raw NO release data was first uniformly converted into part per billion responses (PPB) and the NO release profiles were plotted as NO release in PPB versus time. The NOA instrument calibration constant was used to convert its output signal to moles of NO. In order to calculate experimentally derived MAHMA/NO half-lives, moles of NO is converted to $[MAHMA/NO]_{decomp}$ and finally into $\ln([MAHMA/NO]_{decomp})$. Rate constants were determined by the slope of the linear regression applied to the $\ln([MAHMA/NO]_{decomp})$ versus time graph.

In order to determine the half-life for MAHMA/NO decomposition in PBS, the rate constant determination plots were plotted in terms of percent MAHMA/NO decomposition from 60% to 20% $\ln([MAHMA/NO]_{decomp})$ versus time to achieve a linear fit with an R^2 of 0.999.

Statistical analysis of all experimental data were performed by applying a t-test at the 95% confidence level and comparing its result to the literature value of 60 s to the MAHMA/NO half-life's determined in the 2 mL experiments. All t-tests were performed assuming equal variance and this assumption was validated by a f-test at the 95% confidence level.

2.4 Results

2.4.1 Current State of Chemiluminescence Methodology

The use of chemiluminescence to analysis the NO release from NO donors and NO releasing polymeric materials is routinely done in PBS buffer at pH 7.40 and 37 ºC.[8,9,7,10] Typically, NO release measurements are performed in 2 mL PBS (pH 7.40)

within a custom 2-port sample cell that is deoxygenated prior to NO donor injection. The nitrogen gas is controlled by a gas regulation system that is set to have a bubbler rate of 16 mL/min and a flow rate of 184 mL/min to offset the sampling rate of the headspace for NO at 200 mL/min. Detection of NO occurs within the chemiluminescence chamber, where the NO gas is reacted with ozone. The NO and the ozone gas reacts to creates excited state nitrogen dioxide (NO_2^*) species that when these species relaxes back to the ground state they generate photons. These photons are amplified by the photo multiplier tube, a millivolt response is then measured by a plot computer program. The data is stored on the computer's hard drive. All data processing was performed using Microsoft Excel.

The experimental set-up for measuring NO is shown in Figure 2.1 and features a custom sample cell, a gas regulation system and a gas removal port that leads to the chemiluminescence detector in the NOA instrument.

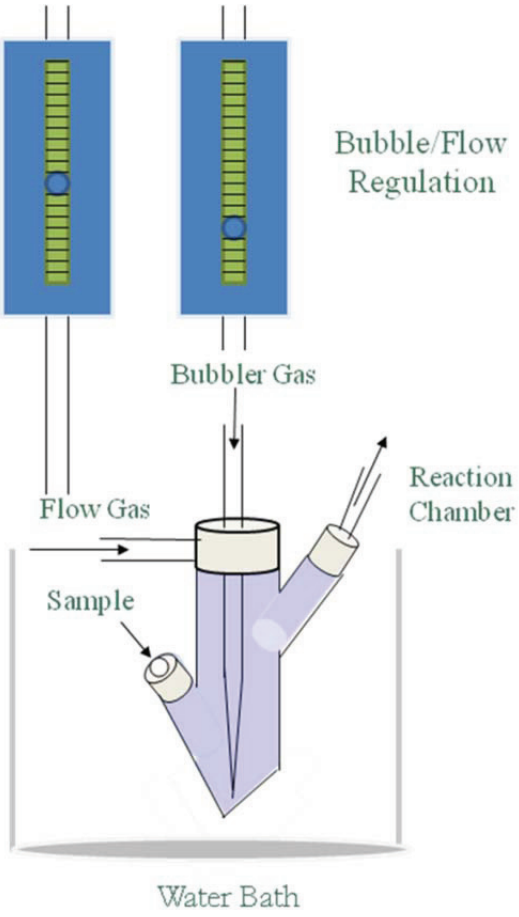

Figure 2.1: A diagram of the NO release measurement set-up with bubble and flow gas entrances (gas regulation), the injection port (sample) and gas removal port (reaction chamber) all labeled.

2.4.2 Chemiluminescence MAHMA/NO Decomposition Studies at 10^{-4} M in 2 mL

To fully assess NO potential role in cell and tissue studies, an NO release measurement method is needed, that is capable of measuring the NO release from a wide range of NO donor concentrations. In these studies, MAHMA/NO will be used as the

model NO donor. Using a spectroscopic method, MAHMA/NO decomposition has been demonstrated to follow first order kinetics (Figure 2.2) and is highly pH dependent.[11,12,6]

$$Rate = k[MAHMA/NO]$$

Figure 2.2: The first order rate law expression for MAHMA/NO decomposition.

The MAHMA/NO decomposition in aqueous environment is shown in Figure 2.3, which produces 2 moles of NO and 1 mole MAHMA. The rate of the reaction, k= 0.0116, has been well-documented in the literature to correspond to a half –life of 60 s for the decomposition of MAHMA/NO.[12,6]

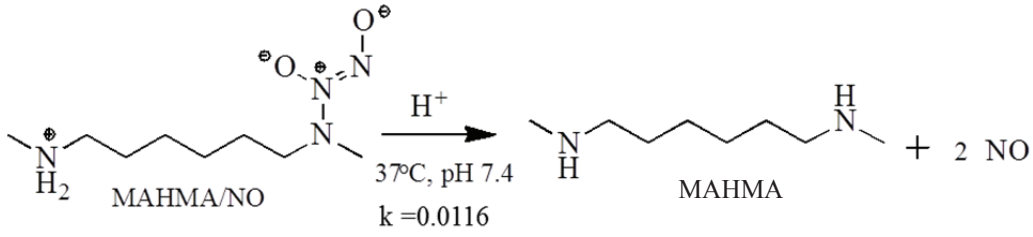

Figure 2.3: The decomposition reaction for MAHMA/NO in aqueous solution at pH 7.4, 37 °C. Based on literature precedent, the rate of reaction has been documented to be k= 0.0116 giving a 60 s half-life for MAHMA/NO.

This reaction will be used to ensure that the method developed is consistent with the previously reported behavior for MAHMA/NO. The reaction shown in Figure 2.3, gives three important factors to gauge the success of this method development: accurate MAHMA/NO half-life, complete NO recovery and standardized reaction conditions (pH 7.4, 37 °C). In this work, MAHMA/NO will used as a model NO donor, to develop a measurement method that allows for detection of NO from lower NO donor concentration than previously reported.

In order to demonstrate that this method is performing properly, three factors have been identified to gauge the performance of this methodology. The first factor is accurate

MAHMA/NO half-lives to ensure that NO release from MAHMA/NO decomposition is first order and has a half-life of 60 s.[12,6] The second factor is obtaining complete NO recovery (100%). The term NO recovery, refers to the experimental total moles of NO divided by the theoretical moles of NO injected and times by 100. This ensures that the total amount of MAHMA/NO injected into the system is proportional to the amount of NO recovered based on 1 mol MAHMA/NO yields 2 mol of NO. Finally, the experimental conditions were standardized to pH 7.40 and 37 °C. Keeping the experimental condition consistent was essential to this methodology because both temperature and pH have been shown to influence the decomposition kinetics of diazeniumdiolates.[6,5]

MAHMA/NO decomposition studies were performed in PBS buffer by measuring NO release with a chemiluminescence detector. The use of chemiluminescence to measure NO release profiles to obtain accurate NO donor kinetics was previously demonstrated with diazeniumdiolates in PBS by Reynolds et al.[13] Figure 2.4A shows the NO release from MAHMA/NO that is characteristic of its decomposition and consistent with previously reported MAHMA/NO decomposition at pH 7.40 and 37 °C. The NO release profile shown in Figure 2.4A can be used to calculate the decomposition rate constant based on first order mechanism where the natural log transformation of $[MAHMA/NO]_{decomp}$ as a function of time is shown in Figure 2.4B. A percent donor decomposition interval (i.e. 60-20%) was applied to eliminate the influence of NO donor mixing at the time of injection until an equilibrium was established and for pH equilibration following the injection of the NO donor in basic solution. The percent donor decomposition interval also increased the linear fit of the trend line applied to calculate

the rate constant for MAHMA/NO decomposition. The half-life of MAHMA/NO calculated using Figure 2.4B yields a half-life of 63±2 s for MAHMA/NO in 2 mL PBS. When compared to the literature value at the 95% confidence interval, it was determined that the experimentally-derived half-lives are within the same sample population as the literature value (60 s). The second qualifier called NO recovery percent was found to be 98±3 demonstrating that the entire NO released from MAHMA/NO was recovered. The third factor was the experimental conditions and the pH was confirmed to pH 7.42±0.02 and the water bath held the buffer at 37 °C. Based on all three factors, the measurement method was determined to be functioning properly for determining accurate MAHMA/NO half-lives and complete NO recovery at pH 7.40 and 37 °C.

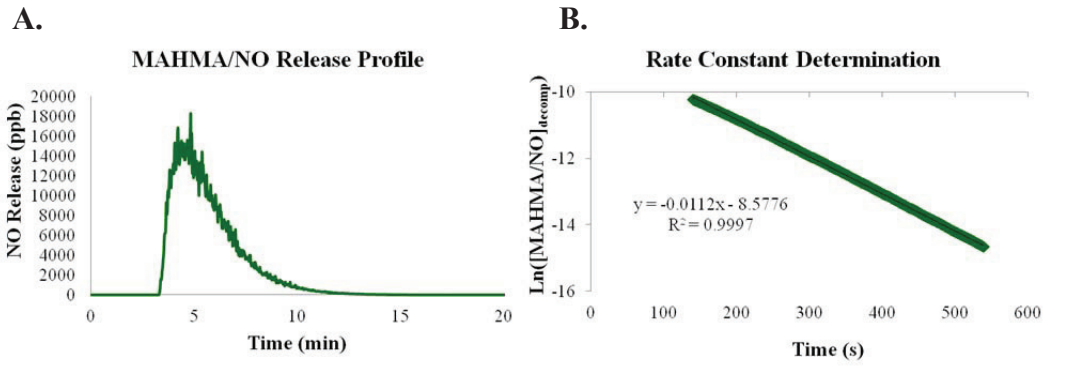

Figure 2.4: Typical NO release profile for MAHMA/NO decomposition (A, left). NO release measurements were converted into ln($[MAHMA/NO]_{decomp}$) to calculate MAHMA/NO half-life (B, right).

2.4.3 Chemiluminescence MAHMA/NO Decomposition Studies at 10^{-4} M in 6, 8 and 10 mL

Although accurate MAHMA/NO half-lives and complete NO recovery were obtained using this measurement method for 10^{-4} M AHMA/NO in 2 mL PBS, the method needed two additional modifications to improve the detection of NO at lower

concentrations of NO donor. The first modification involved increasing the volume of PBS buffer within the sample cell incrementally, and the second involved adjusting the bubbler gas rate using the gas regulation system to achieve total NO recovery and accurate MAHMA/NO half-lives.

After increasing the volume to 6 mL from 2 mL, it was found that the time to recover NO released from a 10^{-4} M MAHMA/NO increased significantly and the experimentally derived MAHMA/NO half-life appeared to slow down. This indicated that there were some potential issues that were preventing accurate MAHMA/NO half-lives from being calculated: 1) donor impurities, 2) donor complexation, 3) change in pH, and or 4) NO trapping in the buffer volume. MAHMA/NO purity was assessed and validated as pure because of a clean UV spectroscopic profile centered at a λ_{max} of 250 nm and ±10% of 100% NO recovery. Donor complexation could be eliminated since MAHMA/NO kinetics were successfully produced in PBS in the literature and in the 2 mL 10^{-4} M MAHMA/NO studies as discussed in section 2.4.2.[6] Changes in pH were discounted because pH was measured before and after each NO release experiment confirming a pH of 7.40. The "apparent" increase in MAHMA/NO half-life was attributed to a large amount of NO remaining in the solution as the buffer volume was increased. An increase in the amount of NO in the buffer volume would lead to "apparently" longer experimentally derived half-lives for MAHMA/NO.

Figure 2.5 gives a visual representation of this explanation where the amount of soluble NO in a 6 mL sample is much larger than in a 2 mL.

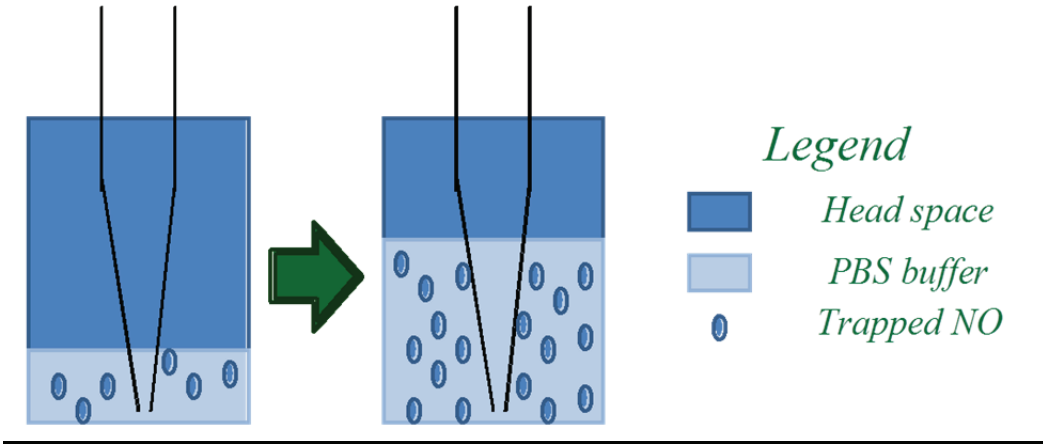

Figure 2.5: As the buffer volume increase from 2 mL to 6 mL the increase in volume allows more NO to be soluble in the buffer, trapping NO and artificially slowing the experimentally derived MAHMA/NO half-lives.

The bubbler rate of 16 mL/min could efficiently purge trapped NO in the 2 mL case; however, the same 16 mL/min bubbler rate was not effective in purging all the trapped NO in large volume studies. As a result as the PBS buffer volume increased within the sample cell, the percent NO recovery for MAHMA/NO would decrease and the half-life would artificially increase, suggesting that indeed the NO gas was being trapped in the buffer. To overcome this, the bubbler gas rate was increased to expel the NO gas trapped within the buffer. As a result, in the 6 mL case the bubbler rate was increased to 35 mL/min to purge NO from the solution into the headspace. By increasing the bubbler rate in larger buffer volume experiments, accurate MAHMA/NO half-lives could be achieved that were similar to those exhibited in the 2 mL volume system discussed in section 2.4.2. Thus, the second modification involved adjusting the bubble gas rate to offset the increase in buffer volume.

In order to understand how the bubbler gas rate was adjusted to yield accurate MAHMA/NO half-lives and complete NO recovery, the gas regulation system will be explained briefly. The gas regulation system controls both the bubbler gas rate and the flow gas rate by using two calibrated flow meter to control both gas rates into the sample cell. This allows for the bubbler and flow gas rates to be balanced to the instrumental sampling rate of 200 mL/min, the amount of gas pulled from the headspace by a vacuum in the NOA. The flow meters were used as shown in Figure 2.2 and were calibrated from 0 to 75.5 mL/min (±1.51 mL/min) [size 1] and 0 to 827.0 mL/min (±16.54 mL/min) [size 2]. The bubbler gas rate was regulated by a size 1 flow meter and the flow gas was regulated by a size 2 flow meter. Each flow meter is calibrated to relate a mL/min rate of gas to a millimeter scale as detailed in Table 2.1.

Table 2.1: Flow Table for Air for 150 mm Flow Meters with Aluminum Ball[14]

Reading at Center of Ball (mm)	Size No. 1 (mL/min)	Size No. 2 (mL/min)
150	75.50	827.0
140	67.30	773.0
130	59.30	719.0
120	52.50	666.0
110	46.00	612.0
100	40.00	556.0
90	34.40	503.0
80	29.20	443.0
70	24.70	380.0
60	20.50	320.0
50	16.70	257.0
40	13.20	200.0
30	10.20	146.0
20	7.50	103.0
10	5.00	69.0
0	0	0

After initial experiments at 2 mL 10^{-4} M MAHMA/NO, studies demonstrated that MAHMA/NO half-lives could be derived reliably from NO release measurements at a donor concentration of 10^{-4} M. The methodology was extended to enable an NO donor concentration of 10^{-4} M at 6, 8 and 10 mL buffer volume. As shown in Table 2.2, by increasing the bubbler gas rate for all the volume studies greater than 2 mL complete NO recovery and accurate MAHMA/NO half-lives were achieved. For 6 mL studies, the bubbler gas was increased to 35 mL/min and experimentally derived half-life for MAHMA/NO was calculated to be 65±2 with an 88±2 percent NO recovery. Again by increasing the bubbler gas to 43 mL/min and 59 mL/min in the 8 mL and 10 mL cases, MAHMA/NO half-lives of 63±2 and 67±9 were calculated with a percent NO recovery of 90±2 and 82±2. By adjusting the bubbler gas rate, both quantitative NO recovery and accurate MAHMA/NO half-lives were achieved in these volume studies.

Table 2.2: Summary of 10^{-4} M MAHMA/NO Decomposition in Different Volumes of PBS[1]

Volume (mL)	Bubble (mL/min)	Flow (mL/min)	% Recovery	Rate Constant	$t_{1/2}$ (s)	Final pH
2	16	184	98±3	0.0110±0.0004	63±2	7.42±0.02
6	35	173	88±1	0.0106±0.0004	65±2	7.42±0.01
8	43	156	90±2	0.0110±0.0006	63±4	7.40±0.03
10	59	140	82±2	0.0105±0.0016	67±9	7.41±0.03

[1] The NO percent recovery, rate constants, half-life and final pH values shown in table are the average value ± the standard deviation (n≥3).

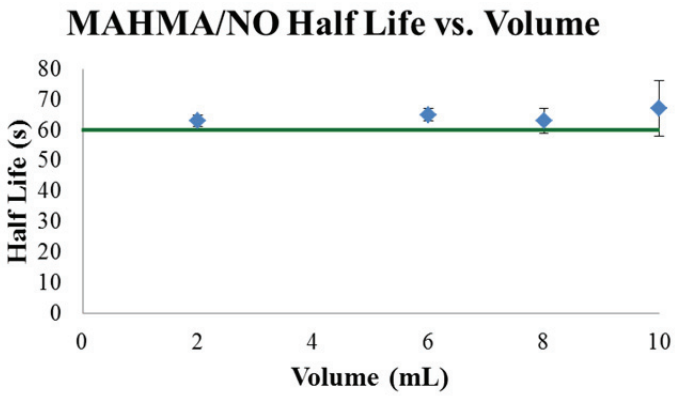

Figure 2.6: Experimental half-lives for MAHMA/NO at different volumes of PBS buffer relative to the literature value for MAHMA/NO, 60 s (solid line).

In order to verify that these experimentally derived half-lives for MAHMA/NO are accurate, they were compared to the literature value previously reported for MAHMA/NO. A comparison of the literature value and the experimentally-derived MAHMA/NO half-lives at different volumes of buffer are summarized in Figure 2.6. Specifically, Figure 2.6 compared the literature value (60 s) to the experimental half-lives calculated for MAHMA/NO at different volumes: 63±2 (2 mL), 65±2 (6 mL), 63±4 (8 mL) and 67±9 (10 mL). Together, Table 2.2 and Figure 2.6 is evidence of a well characterized NO measurement method at various volumes of PBS buffer for 10^{-4} M NO donor concentrations. The experimental conditions at various volumes were adjusted to achieve the same percent NO recovery and accurate MAHMA/NO half-lives as previously demonstrated in the 2 mL 10^{-4} M MAHMA/NO decomposition experiments in section 2.4.2. This assertion has been confirmed through statistical analysis at the 95 % confidence interval comparing the experimentally derived MAHMA/NO decomposition half-lives at the 6, 8 and 10 mL buffer volumes to the experimentally derived MAHMA/NO decomposition half-lives for MAHMA/NO at the 2 mL volume. At the 95

% confidence interval, it was determined that all of the experimental half-lives are within the same population and are consistent with the reported value for MAHMA/NO. These experimental results (Figure 2.6 & Table 2.2) and the statistical analysis demonstrates a measurement method that can obtained accurate MAHMA/NO half-lives and complete NO recovery at pH 7.40 and 37 °C.

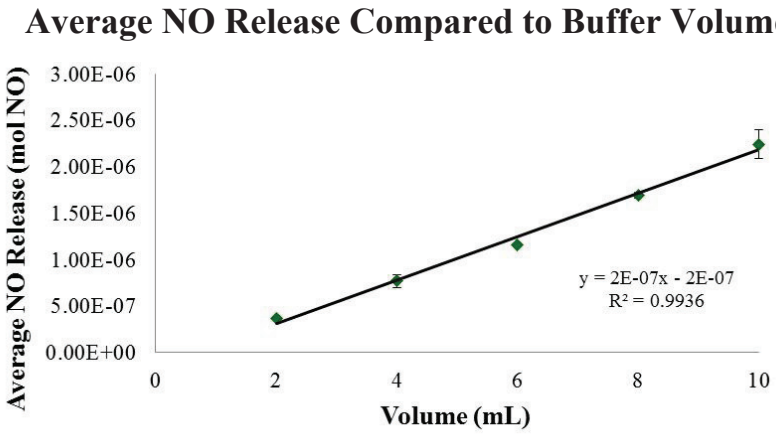

Figure 2.7: The graph shows the average moles of NO released at five different volume of PBS using an 11 mM MAHMA/NO stock. Using a linear regression, the data was fitted achieving a linear fit of $R^2 = 0.9936$.

Further, a comparison of total NO release and buffer volume will be used to determine a relationship between NO release and volume. Figure 2.5 shows a graph that plots the total average moles of NO released from a 11 mM MAHMA/NO stock with respect to different volume of buffer in the sample cell. In these experiments, the buffer volume and the injection volume increase linearly from 20 µl in 2 mL to 100 µl in 10 mL. The linear fit demonstrates that the average moles of NO increase linearly with injection volume and buffer volume with a R^2 of 0.9936. As evident in Figure 2.5, the linearity between the moles of NO released and volume of buffer was confirmed. Since a linear relationship was established between the average NO release and the buffer

volume, the MAHMA/NO half-lives measured at different volumes of buffer could now be compared to each other. The establishment of this relationship between NO release and volume is important for comparing the resultant experimental half-lives to the optimized 2 mL system and to the MAHMA/NO half-life previously reported in the literature.

2.4.4 *Chemiluminescence MAHMA/NO Decomposition Studies at 10^{-7} M in 10 mL*

This section describes NO measurements from 10^{-7} M MAHMA/NO. Using the 10 mL buffer system, a 100 µl aliquot of the MAHMA/NO stock solution was injected into the sample cell. As shown in Figure 2.8A, the NO release profile shows an exponential decay characteristic of the spontaneous decomposition of MAHMA/NO. Since the MAHMA/NO concentration is much more dilute than the 10^{-4} M studies the complete MAHMA/NO decomposition occurs in 500 s versus 20 min.

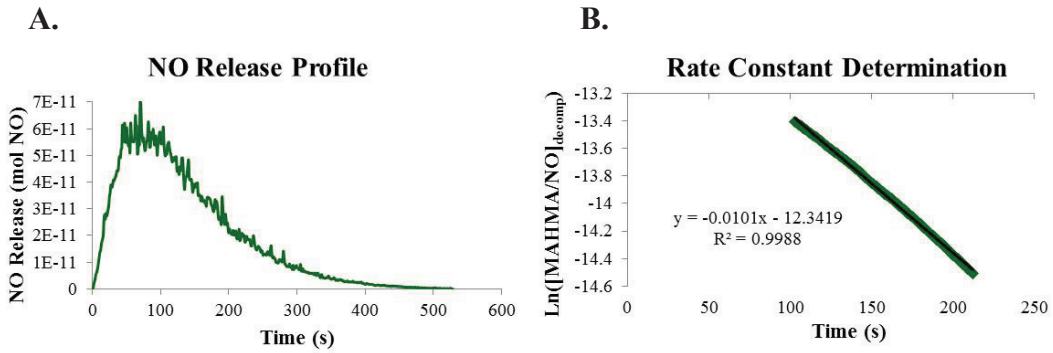

Figure 2.8: Even at more dilute concentration of NO donor, the NO release profile for MAHMA/NO decomposition is conserved although short lived at 500s (left, A). The rate constant determination graph shows rate constant determination using first order kinetics to obtain accurate MAHMA/NO half-lives (right, B).

Further, the MAHMA/NO half-lives determined from a $4.4x10^{-7}$ M MAHMA/NO donor concentration were calculated to be 66±2 with 117±2 NO recovery. The 19% derivation from theoretical NO recovery, is similar to the standard deviation experienced in the 10^{-4} M studies. Statistical analysis was performed at the 95% confidence interval to confirm that these experimentally derived half-lives were within the same population as the literature value for MAHMA/NO. This confirms that through system refinement and modification of the bubbling rates accurate MAHMA/NO decomposition half-lives were achieved and that they were statistically similar to the literature values for MAHMA/NO at the 95% confidence interval. This experiment demonstrates how valuable this new methodology can be for the analysis of NO release from dilute concentration of NO donors because prior chemiluminescence methodology allowed for routine analysis of NO release from 10^{-4} M donor concentrations, now using this methodology the concentration range was extended to 10^{-7} M MAHMA/NO.

Because of the development of the data processing protocol, this method is able to analyze NO release profiles to obtain accurate MAHMA/NO half-lives from 10^{-4} M and 10^{-7} M MAHMA/NO donor concentrations.

Figure 2.9 shows a direct comparison in terms of NO release (mol NO) between the 10^{-4} M MAHMA/NO performed in 2 mL to the 10^{-7} M MAHMA/NO performed in 10 mL.

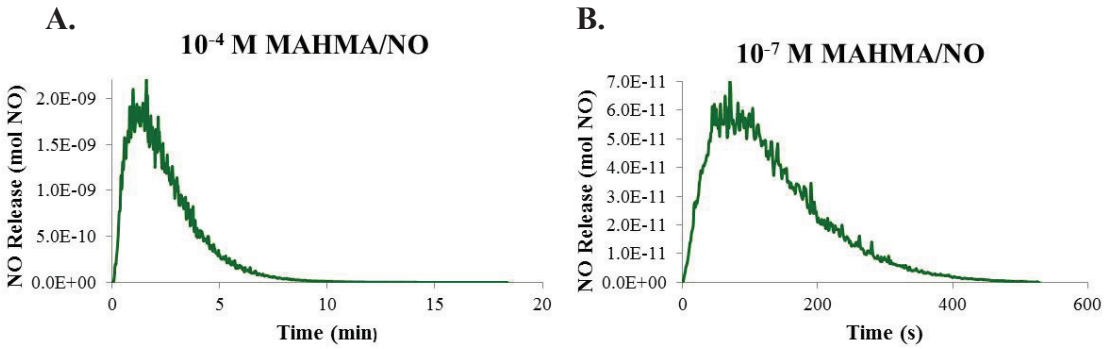

Figure 2.9: A direct comparison of the NO release profiles (moles NO) for the 10^{-4} M MAHMA/NO (A) and 10^{-7} M MAHMA/NO (B).

Using the percent decomposition of 60%-20%, this method is able to generate accurate MAHMA/NO decomposition half-lives for a range of 10^{-4} to 10^{-7} M MAHMA/NO concentrations. Prior to the development of this methodology, 10^{-7} M MAHMA/NO could not be measured using standard chemiluminescence measurement method.

2.5 Conclusions

To conclude, the specific aim of this work was to extend the range NO donor concentrations that could be monitored with chemiluminescence. This methodology was developed using MAHMA/NO at 10^{-4} M that yielded accurate MAHMA/NO decomposition half-lives and complete NO percent recovery at pH 7.40 at 37 °C. Increasing the volume in the sample cell and altering the bubbling gas rate were crucial to monitor NO release from these dilute NO donor concentrations. These modifications allowed for the analysis of a 4.4×10^{-7} M MAHMA/NO donor concentration, which could not be measured previously using other chemiluminescence methods.

2.6 References:

1. Hall, C. N.; Garthwaite, J., What is the real physiological NO concentration in vivo? *Nitric Oxide* **2009,** *21*, 92-103.
2. Yamamoto, T.; Bing, R. J., Nitric Oxide Donors. *Proceedings of the Society for Experimental Biology and Medicine* **2000,** *225*, 200-206.
3. Feelisch, M.; Stamler, J. S., Donors of Nitrogen Oxides. In *Methods in Nitric Oxide Research*, Feelisch, M.; Stamler, J. S., Eds. John Wiley & Sons: New York, 1996; pp 71-115.
4. Wang, P. G.; Xian, M.; Tang, X.; Wu, X.; Wen, Z.; Cai, T.; Janczuk, A. J., Nitric Oxide Donors: Chemical Activities and Biological Applications. *Chemical Reviews* **2002,** *102* (4), 1091-1134.
5. Hrabie, J. A.; Klose, J. R.; Wink, D. A.; Keefer, L. K., New Nitric Oxide-Releasing Zwitterions Derived from Polyamines. *Journal of Organic Chemistry* **1993,** *58* (6), 1472-1476.
6. Davies, K. M.; Wink, D. A.; Saavedra, J. E.; Keefer, L. K., Chemistry of the Diazeniumdiolates. 2. Kinetic and Mechanisms of Dissociation to Nitric Oxide in Aqueous Solution. *Journal of American Chemical Society* **2001,** *123* (23), 5473-5481.
7. Reynolds, M. M.; Hrabie, J. A.; Oh, B. K.; Politis, J. K.; Citro, M. L.; Keefer, L. K.; Meyerhoff, M. E., Nitric Oxide Releasing Polyurethane with Covalently Linked Diazeniumdiolated Secondary Amines. *Biomacromolecules* **2006,** *7* (3), 987-994.
8. Shin, J. H.; Metzger, S. K.; Schoenfisch, M. H., Synthesis of Nitric Oxide-Releasing Silica Nanoparticles. *Journal of American Chemical Society* **2007,** *129* (15), 4612-4619.
9. Reynolds, M. M.; Zhou, Z. Z.; Oh, B. K.; Meyerhoff, M. E., Bis-diazeniumdiolates of Dialkyldiamines: Enhanced Nitric Oxide Loading of Parent Diamines. *Organic Letters* **2005,** *7* (14), 2813-2816.
10. Damodaran, V. B.; Joslin, J. M.; Wold, K. A.; Reynolds, M. M., S-Nitrosated biodegradable polymers for biomedical applications: synthesis, characterization and impact of thiol structure on the physiocochemical properties. *Journal of Material Chemistry* **2012**.
11. Keefer, L. K., Diazeniumdiolate Database. December 28, 2011 ed.
12. Keefer, L. K.; Nims, R. W.; Davies, K. M.; Wink, D. A., "NONOates"(1-Substituted Diazen-1-ium-1,2-diolates) as Nitric Oxide Donors: Convinent Nitric Oxide Dosage Forms. *Methods in Enzymology* **1996,** *268*, 281-293.
13. Reynolds, M. M.; Zhou, Z.; Oh, B. K.; Meyerhoff, M. E., Bis-diazeniumdiolates of Dialkyldiamines: Enhanced Nitric Oxide Loading of Parent Diamines. *Organic Letters* **2005,** *7* (14), 2813-2816.
14. Riteflow Flowmeters and Kits. In *Scienceware*, Bel-art products: Pequannock, NJ, p 14.

3. MEASUREMENT METHOD TO QUANTIFY NO RELEASE FROM NO DONORS IN CARBON DIOXIDE BUFFERED TISSUE MEDIA

3.1 Introduction

Nitric oxide (NO) donors are used to study NO in cell signaling pathways using *in vitro* models. As such, there is a real need to develop new analytical methods capable of analyzing NO release from NO donors in cell and tissue media. Current measurement methods used to monitor NO *in vitro* focus on measuring the byproducts of NO and are not typically performed in real time. To measure NO accurately under *in vitro* conditions, a measurement method is needed that is capable of analyzing NO generated from NO donors in buffered tissue media. As described in Chapter 2, Methylaminehexylmethylamine diazeniumdiolate (MAHMA/NO) was used to develop a NO release measurements method that yield total NO recovery and accurate half-lives for lower NO donor concentrations at pH 7.40 and 37 °C in phosphate buffered saline (PBS). In this chapter, MAHMA/NO will be used again to develop a measurement method that allows for complete NO recovery and accurate MAHMA/NO half-lives in buffered tissue media at pH 7.40 and 37 °C. To ensure the pH is indeed stable the method incorporates a real-time pH measurement probe. Finally, to further demonstrate that this methodology is capable of measure NO release from NO donors under *in vitro* conditions, a 1.5 h NO release profile was collected for diethylenetriamine diazeniumdiolate (DETA/NO) measured in tissue media buffered by carbon dioxide (CO_2).

3.2 Materials

Neurobasal tissue media (Invitrogen, phenol red & L-glutamine free), D-(+)-glucose (Sigma Aldrich, 99.5%), 200 mM L-glutamine (Millipore), and L-glutamic acid (Fisher Scientific, 99.0-100.5%) were purchased comercially. Diethylenetriamine (DETA, Alfa Area, 99%) was purchased for NO donor synthesis, DETA/NO. DETA/NO was synthesized and purified in house following a detailed description described in section 3.3.1. For tissue media incubation experiments, a custom 5% carbon dioxide balanced with 95% nitrogen was purchased from Air Gas. Three pH calibration standards 4.00, 7.00 and 10.00 were purchased from VWR.

3.3 Methods

3.3.1 Nitric Oxide Donor Synthesis

DETA/NO was prepared according to a previously published report and is described in Section 2.3.1.[5] The diazeniumdiolate was spectroscopically characterized for purity by UV spectroscopy at 252 nm.

3.3.2 Real-time pH measurements

All real-time pH analysis were measured using the Accumet Excel XL50 Dual Channel pH/Ion/Conductivity meter, which allowed for 1000 data point storage at a time interval as fast as 3 s. The pH probes that were used when performing the real-time pH analysis were Mettler Toledo In Lab Micro Pro (Ag/AgCl, 3M KCl).

Real-time pH Measurements Experimental Set-up

A custom 3-port NOA sample cell was designed to incorporate a pH probe as shown in Figure 3.1.

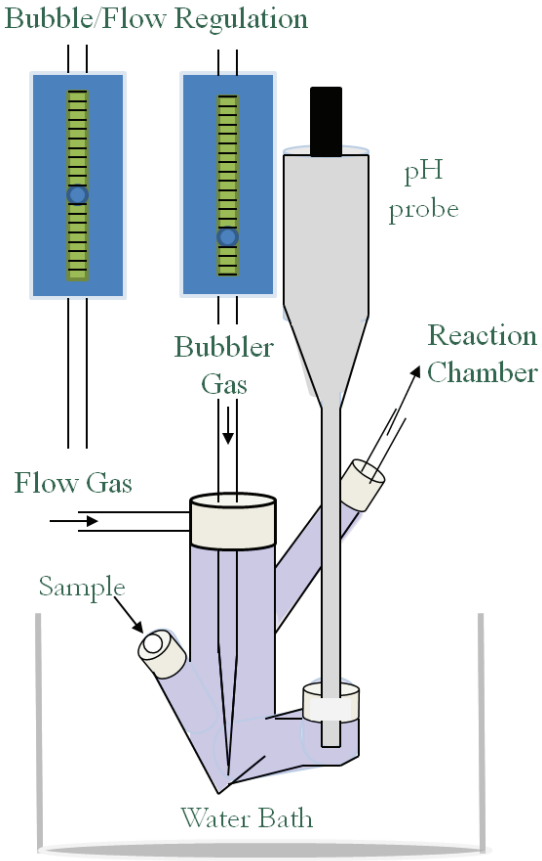

Figure 3.1: A diagram of the NO release measurement set-up with the 3-port custom NOA sample cell with the bubble and flow gas entrances (gas regulation), the injection port (sample), gas removal port (reaction chamber) and the pH probe port all labeled.

The pH probe was oriented vertically within the custom 3-port reaction cell. Prior to insertion, the pH probe was fitted with an o-ring (105, ID 5/32" and OD 11/32"), and a septa vial cap. The pH probe head was submerged in at least by 0.5 cm of the sample solution. All real-time pH data was converted from an .html file to an Excel file and all measurements were processed using Excel.

Evaluation of Custom 3-port Sample Cell and Real-Time pH Measurements by an Acid-Base Titration

The NOA instrument was turned on and 2 mL PBS buffer (pH 7.40) was added to the 3-port custom sample cell. The Mettler Toledo In Lab pH probe was attached to the Accumet Excel XL50 Dual Channel pH meter and calibrated. The pH probe was inserted into the 3-port sample cell as described previously. Real-time pH measurements were setup with a sampling interval of 5 s. Before any acid or base was titrated into the 3-port sample cell, a 24 points (~2 min) baseline was recorded. An aliquot of 50 µl of 0.1 M HCl was injected into the sample inlet and the pH was recorded for 60 points (5 min). A total of nine injections shown in Table 3.1 were made to evaluate pH response of the pH probe under NO release measurement conditions.

Table 3.1: Acid and Base Titration Injection Volumes

Injection	Volume (µl)	Acid/Base	Injection Time Point
1	50	HCl	25
2	100	NaOH	85
3	100	HCl	145
4	100	NaOH	205
5	100	HCl	267
6	200	NaOH	327
7	200	HCl	387
8	100	NaOH	447
9	250	HCl	507

3.3.3 Tissue Media Preparation

Fresh tissue media was prepared prior to each experiment to ensure freshness and proper buffering of the media. A 2.5 mM L-glutamic acid solution and a 45% glucose solution were prepared in 10 mL of Millipore treated water. Both solutions were stored in for 1 month at 4 °C. In order to make a 100 mL tissue media, the following reagents were mixed together 97.63 mL Neurobasal media, 1 mL 2.5 mM L-glutamic acid, 1.1 mL 45% glucose, and 248 µl 200 mM glutamine.

3.3.4 Nitric Oxide Release Measurements

Nitric oxide release measurements were performed as described in section 2.3.2.

3-port sample cell NO release experiment

Nitric oxide release experiments were performed using the 3-port sample cell at the 8 mL buffer volume. These NO release experiments were performed as previously described in section 2.3.2 with a 11.8 mM MAHMA/NO stock.

NO release experiments from 10^{-4} M MAHMA/NO decomposition in buffered tissue media

Nitric oxide release experiments were performed as described previously in section 2.3.2, in 2 mL tissue media using the 3-port sample cell and with other minor modifications details below. The tissue media was buffered to pH ~7.40 with 5% CO_2 gas at a bubbler gas rate of 20 mL/min rate and a flow gas rate of 178.4 mL/min. Real-time pH measurement were setup as described in section 3.3.2 at a sampling interval of 10 s. The data collection for pH and NO release began as soon as 5% CO_2 encounters the tissue media and then, was continued for 1.5 h to ensure that the pH of the tissue media was buffered to pH ~7.40. Once the pH stabilized, a 20 µl from either a 10.5 mM or a

13.9 mM MAHMA/NO solution prepared in 0.01 M NaOH was injected into the sample cell. The NO release and real-time pH data were processed using Excel as described in section 2.3.2 and 3.2.2, respectively.

NO release experiments from DETA/NO decomposition in buffered tissue media

Nitric oxide release experiments were performed in 2 mL tissue media just like the previous 10^{-4} M MAHMA/NO experiment. After the tissue media was buffered to pH 7.40 using 5% CO_2 at a bubbler gas rate of 20 mL/min for approximately ~ 1 h, a 20 µl aliquot of a 60 mM DETA/NO in 0.01 M NaOH stock was injected into the 3-port sample cell and NO release was measured for 1.5 h. The NO release and real-time pH data were processed using Excel as described in section 2.3.2 and 3.2.2, respectively.

3.4 Results

3.4.1 Method optimization to enable NO release measurement from MAHMA/NO decomposition in buffered tissue media

The aim is to development a measurement method that can monitor NO release from NO donors in buffered tissue media at 37 °C and pH 7.40. This is, in contrast to the PBS buffer experiments where the buffer range and capacity did not require an additional reagent to maintain pH 7.40. However, in the tissue media experiments 5% CO_2 is used to buffer the tissue media by employing carbonic acid and bicarbonate buffering system. As in the previous chapter, MAHMA/NO NO recovery and MAHMA/NO half-lives will be used as a criteria to develop a NO release measurement system in tissue media buffered by CO_2 at 37 °C.

This methodology is similar to the PBS experiments presented in Chapter 2, however, there are three major modifications that are needed to measure NO release from

MAHMA/NO in tissue media, pH 7.4. These modifications include: a) the incorporation of a pH probe for real-time pH measurements, b) the use of tissue media and c) the use of 5% CO_2 to buffer the pH of the media. Care was taken to avoid potential issues that could influence the NO recovery or the experimentally derived MAHMA/NO half-lives. These potential problems include: donor interaction with compounds in tissue media, ability to achieve, maintain and monitor stable pH through addition of CO_2 and scavenging of NO by components within the tissue media. The biggest challenge was maintaining a constant pH of the tissue media. As discussed in Chapter 2, three factors will be used to certify the performance of this measurement method in buffered tissue media. These three factors are obtaining accurate MAHMA/NO half-lives, theoretical NO recovery and maintenance standardized experimental conditions (pH 7.40, 37 °C).

The incorporation of a micro pH probe into the experimental set-up as depicted in Figure 3.1 was designed to measure real-time pH measurements within the 3-port sample cell as the NO release measurements were collected. Further the pH probe was used to help determine the proper flow rate for 5% CO_2 to adequately buffer the tissue media to pH 7.4±0.1. This created a dual system that could monitor both the NO release from MAHMA/NO decomposition and also, ensure that pH 7.4 was maintained. The addition of a pH probe required a new 3-port custom sample cell be designed. Each port was designed to have a specific function to ensure that the measurements recorded within the sample cell are accurate and reproducible. The aim of the design was to 1) facilitate the incorporation of a pH probe into the cell, 2) not interfere with the amount of volume of buffer in the cell and 3) to create a sample cell that functions exactly the same as the 2-port reaction cell used previously to collect NO release measurements. Finally, two

custom cells were designed to enable real-time pH measurement and NO release in two buffer volume ranges, small (2,4,6) and larger (8, 10) (Figure 3.2B,C).

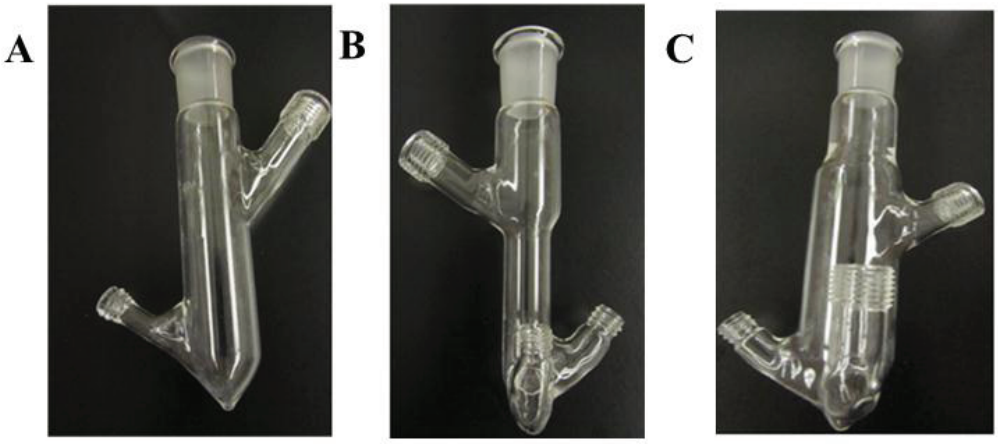

Figure 3.2: A comparison of the standard 2-port small volume NOA cell (left, A) and the custom 3-port in two sizes, small volume NOA cell (center, B) and large volume NOA cell (left, C).

To ensure that the change from the 2-port to the 3-port sample cell did not influence the half-lives of MAHMA/NO decomposition, a control experiment was designed. A comparison of MAHMA/NO half-lives calculated from NO release data derived from 8 mL PBS in the 3-port sample cells with the MAHMA/NO decomposition kinetics obtained in the 2 mL 2-port sample cell was performed. Previously in section 2.4.2, this 2 mL experiment proved to be statistically similar at the 95% confidence interval with the 60 s reported value for MAHMA/NO. The 3-port 8 mL experiments were preformed exactly as the 2-port experiment discussed in section 2.3.2. Table 3.2 show a comparison of the experimental data produced using the 2mL 2-port and the 8 mL 3-port sample cells. Using the 3-port sample cell, MAHMA/NO half-lives of 68±2 were calculated and compared to the MAHMA/NO half-lives 63±4 from 10^{-4} M MAHMA/NO experiment in the 2-port sample cell. This comparison indicated that the addition of the third port into

the sample cell did not influence the MAHMA/NO kinetics. At the 99% confidence interval, these MAHMA/NO half-lives were determined to be statistically similar to each other and to the report literature value for MAHMA/NO.

Table 3.2: Evaluating the Function of 3-port Sample Cell to the 2-port Sample Cell by Comparing Experimentally Derived MAHMA/NO Half-Lives

Reaction cell	Rate Constants	$t_{1/2}$ (s)
2-port	-0.0110±0.0004	63±4
3-port	-0.0102±0.0002	68±2

Another important design consideration when designing for the sample cell for the integration of a pH probe was that the pH probe needed to be oriented vertically to produce the most accurate readings. Real-time pH measurements are extremely important to this measurement method because NO is derived from diazeniumdiolates and their decomposition is highly dependent on pH.[6] To evaluate the responds time of the pH probe, a qualitative experiment was performed by titrating multiple injection volumes of 0.1 M NaOH and HCl into 2 mL PBS.

As shown in Figure 3.3, the real-time pH response of the pH probe integrated into the NOA cell was rapid after multiple injection of either 0.1 M HCl (red) or 0.1 M NaOH (blue). This confirmed the pH probe's ability to function while integrated into the NOA cell and to be used to monitor the real-time pH in the tissue media experiments.

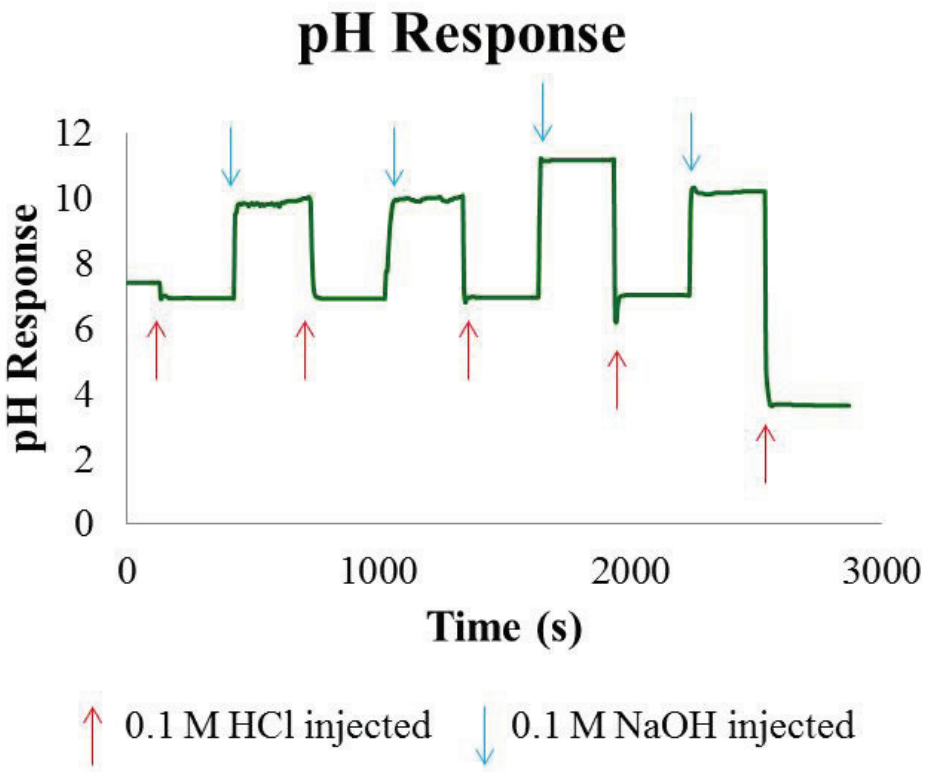

Figure 3.3: A graph shows the real-time pH response of the pH probe following different injection volumes of 0.1 M NaOH (blue) and 0.1 M HCl (red).

3.4.2 NO release measurements from 10^{-4} M MAHMA/NO in buffered tissue media

Many *in vitro* studies using cell and tissue models are used to understand NO role in cellular behaviors, but no detection method exists for monitoring NO release in buffered tissue media. Three major modifications will be needed to transition from a PBS system to a buffered tissue media system at pH 7.40 and 37 °C. The first is to transition the system from PBS buffer to Neurobasal tissue media. One challenge, in particular with

Neurobasal tissue media is that there is a large increase in the number and variety of species that could react or interfere with accurately measuring NO. The second major difference in the experimental protocol was the use of 5% CO_2 in 95% nitrogen instead of 100% nitrogen as the bubble and flow gas used in all previous NO release experiments. The third was real-time pH achieved through the incorporating a pH probe into the custom 3-port sample cell. These three changes will enable this measurement method to record real-time NO release measurement from NO donors in a CO_2 buffered tissue media environment.

In order to incorporate the needed amount of 5% CO_2 to maintain the tissue media at pH 7.40, a pH probe was used to determine the appropriate flow rate of 5% CO_2 by recording real-time pH measurements. A bubbler gas rate of 5% CO_2 was needed to be experimentally determined and maintain the pH 7.4 ± 0.1 of the tissue media prior to the injection of NO donor. The bubbler gas rate was determined to be 20 mL/min (178 mL/min) to buffer 2 mL of tissue media at pH ~7.40. Figure 3.4 shows the pH response once 20 mL/min of 5% CO_2 was added to 2 mL tissue media. There is an immediate pH response to the 5% CO_2 and the pH stabilizes at approximately pH ~7.40 after 30 min. The pH response was monitored for 1.5 h prior to injecting 20 µl of MAHMA/NO solution into the buffered tissue media to collect NO release from MAHMA/NO decomposition to ensure that the pH was indeed stable. The NO release data was converted to MAHMA/NO half-lives using first order kinetics.

Table 3.3 shows a summary of results from 10^{-4} M MAHMA/NO experiments in both PBS and Tissue Media at 2 mL volume.

Table 3.3: Evaluating the Difference in Aqueous Environments on MAHMA/NO Half-Lives and NO Recovery at pH 7.40, 37 °C

Name	% Recovery	Rate Constant	$t_{1/2}$	Final pH
2mL PBS	98±3	-0.0110±0.0004	63±4	7.48±0.02
2 mL Tissue Media	99±8	-0.00102±0.0006	68±5	7.39±0.03

By comparing the MAHMA/NO decomposition half-lives in tissue media to PBS (pH 7.4), the experimentally derived MAHMA/NO half-lives in tissue media and PBS buffer are very similar to each other. In tissue media, MAHMA/NO half-lives were found to be 68±5 with 99±8 percent NO recovery. When statistical analysis was performed between the experimentally derived MAHMA/NO half-lives in 2 mL PBS and 2 mL buffered tissue media, the half-lives were determined to be statistically similar at the 95% confidence interval. Since the MAHMA/NO half-lives were not change significantly, it can be concluded that the tissue media is not influencing MAHMA/NO decomposition. These experiments also shows that all of the theoretical NO released from MAHMA/NO was detected based on the spectroscopic concentration of MAHMA/NO. The NO recovery for these experiments was 99±8 percent. The complete NO recovery indicates that NO is not interacting with the species in the tissue media as there was no loss in total NO recovery detected by the instrument.

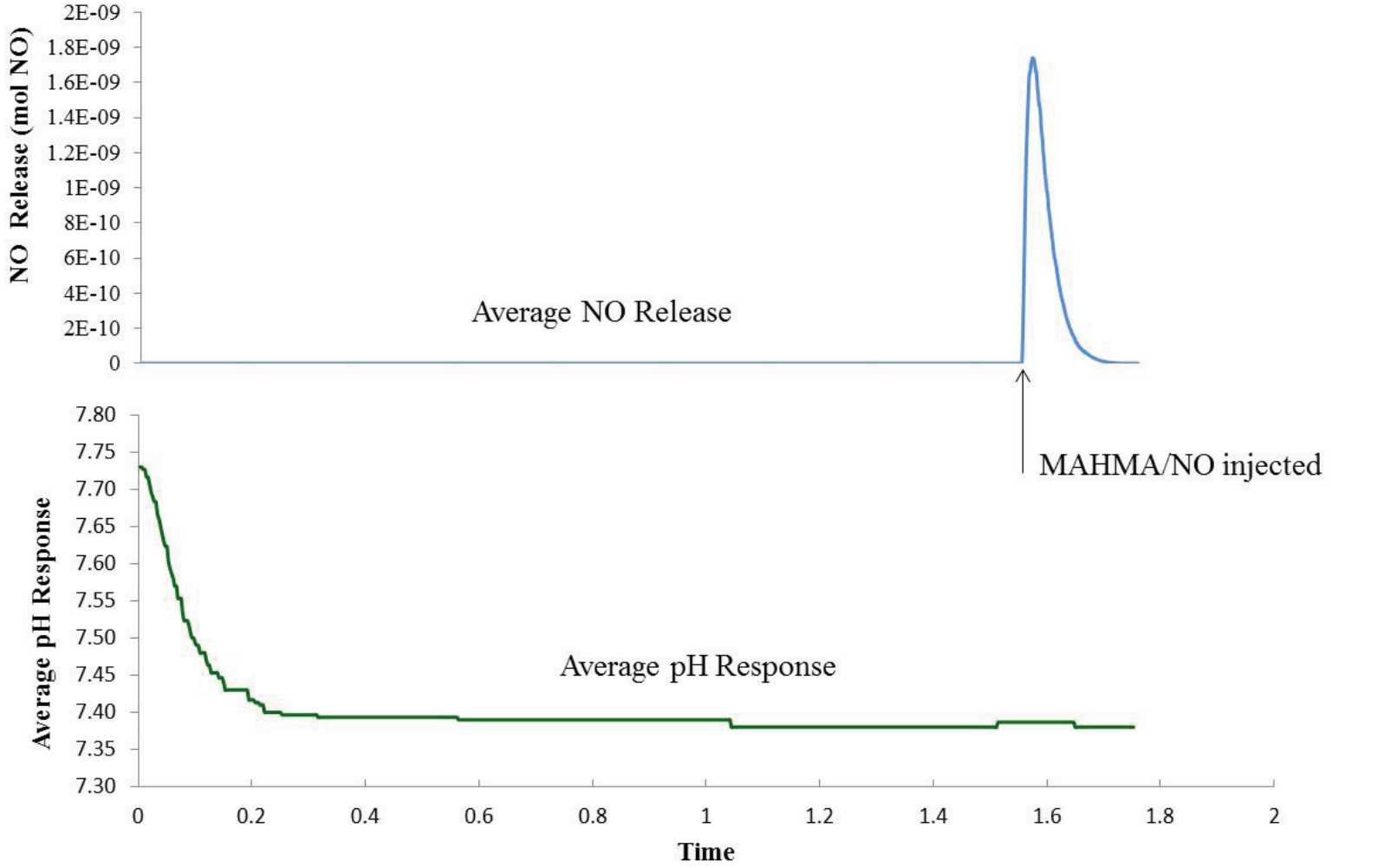

Figure 3.4: This figure shows the average pH response for addition of 5% carbon dioxide at 20 mL/min to the tissue media. After 1.6 h, 20 µl of 11 mM MAHMA/NO solution was injected and NO release is observed from MAHMA/NO decomposition.

This is in contrast to an electrochemical detection method reported by Garthwaite et al. where total NO recovery was not demonstrated in tissue media.[7] In the Garthwiate study, they observed a loss in NO recovery, which was attributed to consumption of NO through the formation of superoxide that converts NO in to peroxynitrite ($ONOO^-$) in the Nuerobasal tissue media. I hypothesize that since the sample cell was deoxygenated in order to use chemiluminescence detection prior to MAHMA/NO injection. The removal of oxygen in the sample cell, allows this measurement method to detect the theoretical amount of NO in buffered tissue media. The removal of oxygen is a likely reason for differences in total NO recovery in these experiments and electrochemical studies where superoxide was proposed to be produced and scavenge NO in the Neurobasal tissue media. The superoxides was proposed to be produced by the interaction of oxygen with riboflavin or through the autooxidation of oxygen by a metal ion.[7] Thus, the total NO recovery with the developed measurement method at 10^{-4} M provides an advantage over previously reported NO detection methods in tissue media.

3.4.3 NO release Experiments with DETA/NO in Buffered Tissue Media

To demonstrate the versatility of this measurement method, another NO donor was used. DETA/NO has a half-life of 20 h, which is different than MAHMA/NO. This diazeniumdiolate decomposes by the same mechanism as MAHMA/NO, where 1 mol of DETA/NO yields 2 moles of NO and 1 mol parent amine, DETA, shown in Figure 3.5.

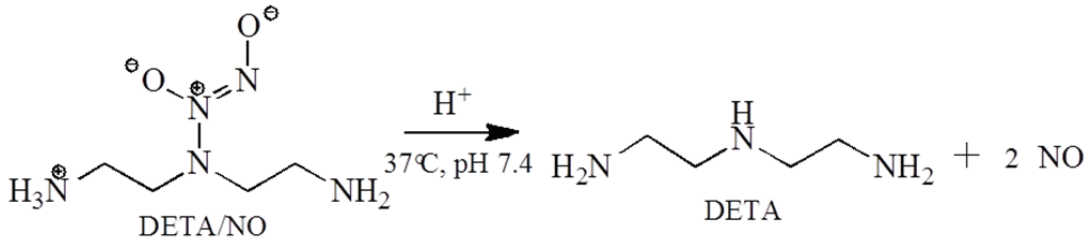

Figure 3.5: The decomposition reaction for DETA/NO in aqueous solution at pH 7.4, 37 °C.

The longer half-life for DETA/NO allows us the ability to examine steady state NO release rates. DETA/NO's release rate may be within the physiologically release range for NO in brain tissue, established to be 1800 to 0.38 nM.[8]

The experiment was performed by preparing fresh tissue media and adding 2 mL to the 3-port custom sample cell. NO release measurements were measured at a 1 s data collection and pH response measurements were collected at 10 s interval. The tissue media was buffered to pH 7.4±0.1 at a 20 mL/min rate of 5% CO_2 and after 1 h, the pH stabilized to pH ~ 7.40 allowing 20 µl of a 60 mM DETA/NO stock to be injected into the buffered tissue media. The NO release profile for DETA/NO is shown in Figure 3.6, along with the pH response following the injection of DETA/NO in tissue media. After the injection of 20 µl of a 60 mM DETA/NO solution, a steady-state release profile is observed over the 1.5 h. The pH response after injection stayed at pH ~7.4 for the entire 1.5 h timeframe. The total average NO release from DETA/NO in 1.5 h was 0.12 ±0.02 nmol. The NO release per s from DETA/NO averaged over the 1.5 h release was calculated to be 22 ±3 fmol/s. This NO release from DETA/NO decomposition may prove useful in probing the effect of lower concentrations of NO donor used in cell and tissue models. The NO release from DETA/NO decomposition showed that other NO donors can be analyzed using this measurement method and that longer experiments do not adversely influence the buffering pH of the tissue media.

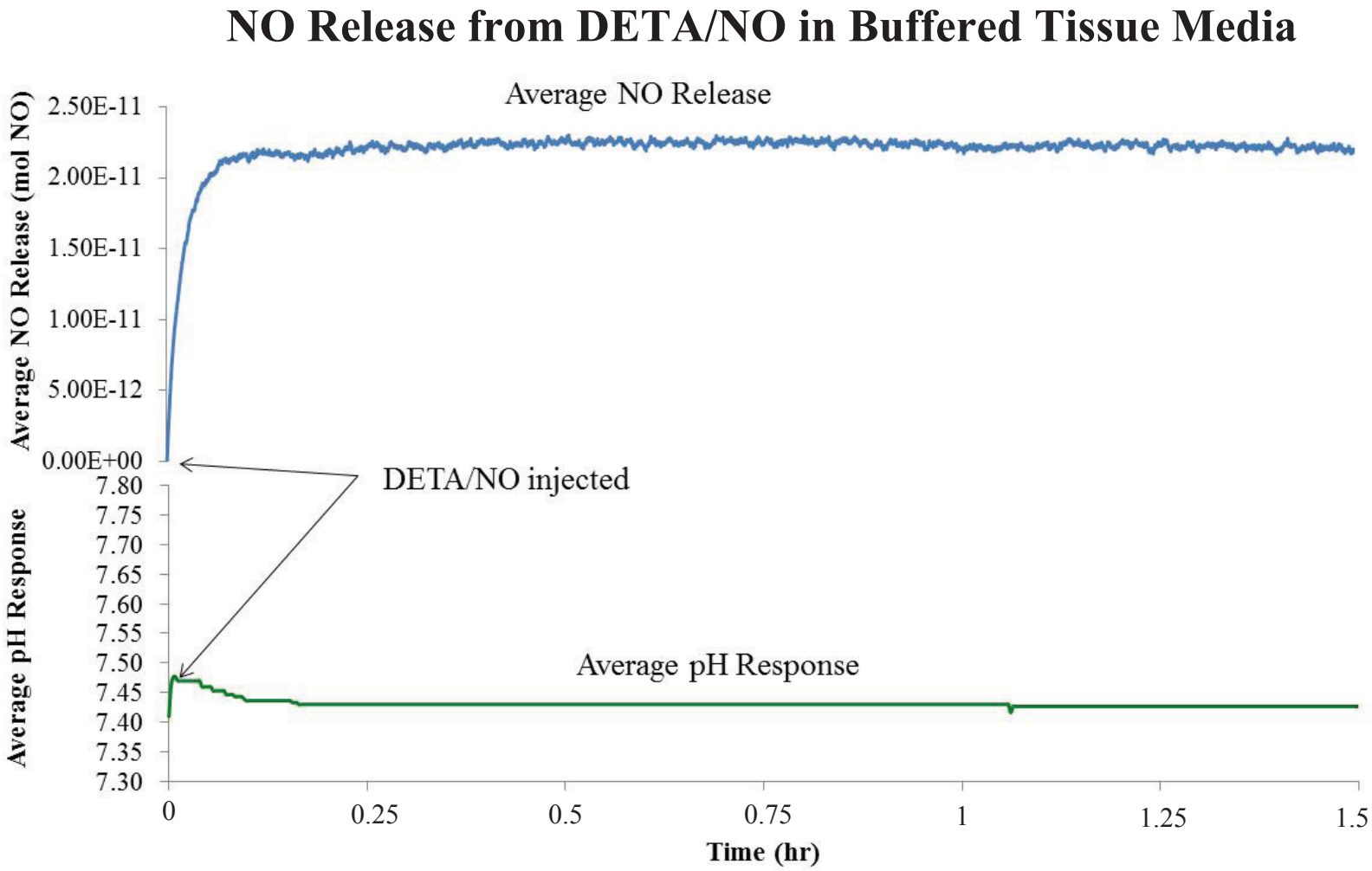

Figure 3.6: This figure shows the average pH response following a 20 µl injection of 60 mM DETA/NO and the NO release profile from DETA/NO decomposition for 1.5 hr.

3.5 Conclusions

In conclusion, I have demonstrated a complete measurement method that combines real-time pH and NO release measurement to measure NO from NO donor decomposition through NO release in buffered tissue media. This measurement method demonstrates the first analytical method to allow for NO release measurements in CO_2 buffered tissue media (pH 7.40, 37 °C) mimicking *in vitro* conditions. These measurements were enabled by the design of a custom 3-port sample cell to integrate a pH probe, which determine the proper bubbling rate of 5% CO_2 to effectively buffer the Neurobasal tissue media at pH 7.40±0.1. This measurement method also, allowed accurate MAHMA/NO half-lives to be experimentally derived in 2 mL buffered tissue media finding that these experimentally derived half-lives were statistically similar at the 95% confidence interval to the 60 s literature reported value for MAHMA/NO. Finally, this novel measurement method was shown to be effective in monitoring NO release from multiple NO donor, specifically, MAHMA/NO and DETA/NO, under simulated *in vitro* conditions.

3.6 References

1. Saavedra, J. E.; Keefer, L. K., Nitrogen-Based Diazeniumdiolates: Versatile Nitric Oxide-Releasing Compounds in Biomedical Research and Potential Clinical Applications. *Journal of Chemical Education* **2002,** *79* (12), 1427-1434.
2. Pulfer, S. K.; Ott, D.; Smith, D. J., Incorperation of nitric oxide-release crosslinked polyethyleneimine microspheres into vascular grafts. *Journal of Biomedical Material Research* **1997,** *37* (2), 182-189.
3. Yoon, J. H.; Wu, C. J.; Homme, J.; Tuch, R. J.; Wolff, R. G.; Topol, E. J.; Lincoff, A. M., Local Delivery of Nitirc Oxide from an Eluting Stent to Inhibit Neointimal Thickening in a Pocine Coronary Injury Model. *Yonsei Medical Journal* **2002,** *43* (2), 242-251.
4. Reynolds, M. M.; Frost, M. C.; Meyerhoff, Nitric Oxide-Releasing Hydrophobic Polymers: Preparation, Characterization and Potential Biomedical Applications. *Free Radical Biology and Medicine* **2004,** *37* (7), 926-936.
5. Hrabie, J. A.; Klose, J. R.; Wink, D. A.; Keefer, L. K., New Nitric Oxide-Releasing Zwitterions Derived from Polyamines. *Journal of Organic Chemistry* **1993,** *58* (6), 1472-1476.
6. Davies, K. M.; Wink, D. A.; Saavedra, J. E.; Keefer, L. K., Chemistry of the Diazeniumdiolates. 2. Kinetic and Mechanisms of Dissociation to Nitric Oxide in Aqueous Solution. *Journal of American Chemical Society* **2001,** *123* (23), 5473-5481.
7. Keynes, R. G.; Griffiths, C.; Garthwaite, J., Superoxide-dependent consumption of nitric oxide in biological media may confound in vitro experiments. *Biochemical Journal* **2003,** *369*, 399-406.
8. Hall, C. N.; Garthwaite, J., What is the real physiological NO concentration in vivo? *Nitric Oxide* **2009,** *21*, 92-103.

4. FUTURE DIRECTION

4.1 Future Directions

The work presented in this thesis, focused on designing a measurement method that enabled measuring nitric oxide (NO) release from a wider range of NO donor concentrations, specifically measuring 10^{-4} M to 10^{-7} M MAHMA/NO donor concentrations. This measurement method may assist researchers in understanding NO's role in physiology by offering greater insight to how NO concentration effect it's biological activity. The second aim for developing this measurement method was to measure NO release from NO donor in carbon dioxide (CO_2) buffered tissue media. However, developing better analytical methods does not end with these two measurement methods for measuring NO. I believe that there are many important questions that could still be addressed using this work is as a starting place. There are three important ideas that could be explored further to improve these NO measurement methods and to use these methods to better understand NO role in physiology.

The first idea would be to further extend the concentration range for monitoring NO release from NO donor solution in the PBS system from 10^{-7} M to 10^{-9} M. An application of this measurement method is to achieve NO release from NO donors that matches specific concentration target for physiological levels of NO releases. These levels of NO release are typically achieved by using dilute NO donor concentrations. Thus, it is relevant to measure even more dilute NO donor concentrations. From the studies presented in Chapter 2, there were two modifications made to the chemiluminescence method to monitor NO release from a $4.4x10^{-7}$ M MAHMA/NO solution: adjusting the bubbler gas rate and increasing buffer

volume in the sample cell. Measuring NO release from $4.4x10^{-7}$ M MAHMA/NO in the 10 mL buffer volume, a 59 mL/min bubbler flow rate was used. This bubbler gas rate almost exceeded the flow capacity for the size 1 flow meter. In order to increase the bubbler gas rate above 75.5 mL/min, a size 2 calibrated flow meter would be needed to modulate the bubbler flow gas for larger volumes of buffer. As the volume within the sample cell increases, additional circulation of the buffer within the sample cell may be needed through the addition of a stir bar or mechanical accessory. This will allow the measurement method to maintain accurate NO recovery, accurate MAHMA/NO half-lives and eliminate the effects of NO trapping, discussed in section 2.4.3. Provided that one can maintain accurate NO recovery and MAHMA/NO half-lives, this method has great potential for monitoring NO release from even lower concentrations of NO donors.

The second idea would be to monitor 10^{-7} M MAHMA/NO donor decomposition in CO_2 buffered tissue media. As demonstrated in Chapter 3, MAHMA/NO and DETA/NO decomposition could be successfully monitored in 2 mL tissue media at 37 °C and pH 7.40 by measuring NO release. Quantification of the theoretical NO recovery and accurate MAHMA/NO half-lives were obtained in the 10^{-4} M MAHMA/NO experiments. Chapter 2, showed that NO release could be measured in 10 mL PBS from 10^{-7} M MAHMA/NO decomposition, while achieving accurate MAHMA/NO half-lives and complete NO recovery. To enable detection of NO release in buffered tissue media, the tissue media would need to be increased from 2 mL to 10 mL. Using the bubbler gas rate determined in chapter 2 as a guide for determining the optimal bubbler rate conditions, the 10 mL tissue media

method would need to be optimized at the 10^{-4} M MAHMA/NO condition to maintain stable experimental conditions (pH 7.40, 37 °C). This bubbler rate would need to be evaluated to maintain pH 7.4±0.1 and yield accurate MAHMA/NO half-lives. A major challenge arose in the preliminary work to optimize this measurement method to monitor NO release from 10^{-7} M MAHMA/NO in buffered tissue media system and the challenge was that at 10^{-7} M MAHMA/NO, a significant drop in NO recovery was observed. A loss in NO recovery had not been observed in the 10^{-4} M MAHMA/NO studies. Figure 4.1 shows a comparison in the NO release from 10^{-7} M MAHMA/NO in the buffered tissue media (Figure 4.1A) and PBS (Figure 4.1 B). The NO release from 10^{-7} M MAHMA/NO in buffered tissue media (Figure 4.1A) was an order of magnitude lower than the NO release observed in the 10^{-7} M MAHMA/NO decomposition in PBS (Figure 4.1B).

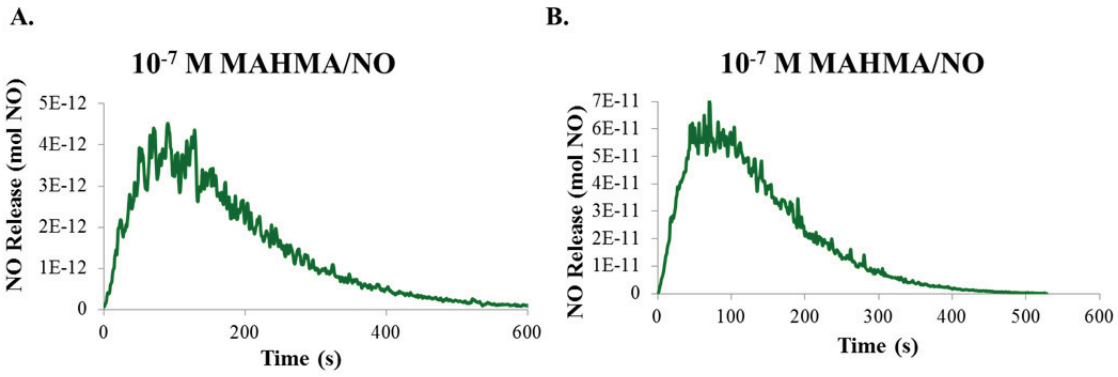

Figure 4.1: A direct comparison of the NO release profile in terms of mol NO for the 10^{-7} M MAHMA/NO in buffered tissue (A) and 10^{-7} M MAHMA/NO in PBS (B).

The experimentally measured NO recovery for NO release from 10^{-7} M MAHMA/NO in buffered tissue media was found to be 8±2. This NO recovery is significantly less than the 99±8 found in buffered tissue media at 10^{-4} M MAHMA/NO in section 3.4.2. This is also

significantly different at the 95% confidence interval, than the NO recovery of 117±2 observed in the 10^{-7} M MAHMA/NO PBS studies. As discussed briefly in Chapter 3, there is a literature precedent by Garthwaite and colleagues for NO consumption in tissue media, specifically implicating Neurobasal tissue media.[1] Neurobasal tissue media is the media used in all of the tissue media experiments presented in this work. In the electrochemical detection method for NO in Neurobasal tissue media, Garthwaite et al. reports a loss in NO recovery that was due to scavenging of NO by components within the tissue media. Specifically, they attribute the loss of NO recovery to NO conversion to peroxynitrite ($ONOO^-$) by superoxide formed from oxygen (O_2).[1] In the 10^{-4} M MAHMA/NO studies in buffered tissue media, accurate NO recovery was observed and I attributed the complete NO recovery to the deoxygenation of the sample cell prior to donor injection. The deoxygenation of the cell would limit the formation of superoxide by preventing NO conversion to $ONOO^-$. However, when the concentration of MAHMA/NO decreased significantly from 10^{-4} M to 10^{-7} M in preliminary studies, a significant loss of NO recovery was observed indicating that deoxygenation of the sample cell may not be enough when analyzing more dilute concentrations of NO donor, like 10^{-7} M. I hypothesize the loss of NO recovery was due to there being ample O_2 within the 100 μl injection volume, this resulted in a significant decrease in the total mol of NO detected. A possible way to increase the amount of NO measured in the 10^{-7} M MAHMA/NO studies in buffered tissue media is to deoxygenate the MAHMA/NO solution prior to NO donor injection into the sample cell. This will removal excess oxygen and be a good control to see if accurate NO recovery could be restored. Prior

to increasing the concentration range of NO donor measured with this method, total NO recovery must be achieved in order to monitor dilute NO donor concentration in CO_2 buffered tissue media.

The establishment of NO release measurements from NO donor decomposition in tissue media allows this measurement method to be used to study the effect of NO on cellular migration in brain tissue by using NO release profiles from the NO donor. MAHMA/NO and DETA/NO established that NO release profiles for the NO donor decomposition could be obtained in buffered tissue media. However, ideally it be interesting to produce a wide range of NO release profile with different relative concentration rates for NO release. These different concentrations of NO from different NO donors could be used to screen *in vitro* cell and tissue models for the effect of NO. These experiments could reveal more about NO's physiological effects. Using this measurement method, NO release profiles could be measured over a 1.5 h to customize NO donor concentrations, that would demonstrate NO release that is within the general physiological concentration of NO previously established to range from 1μM to 100 pM.[2] The measurement method described in this thesis has been developed as a straight forward, bench-top real-time NO release measurement method capable of measuring NO release from NO donors in buffered tissue media. To measure NO release from NO donor in buffered tissue media, it is important to accurately buffer the tissue media with CO_2 to pH 7.40±0.1.

A potential application for this methodology is to look at developing NO release profiles from NO donors that are specifically within the physiological range in the brain from

1800 nM to 0.38 nM.[2] Then use these NO release profiles to better understand the role NO plays in cellular migration with respect to NO concentration. The determination of NO release over a required 1.5 h was successful for DETA/NO, yielding a total NO delivery of 0.6 ±0.1 nM in 1.5 h. The total NO recovery for DETA/NO over 1.5 h was within the targeted physiological range previously reported in the literature for *in vivo* NO release in brain tissue.[1] The NO release rates from DETA/NO decomposition (average mol NO per s) over a 1.5 h release was calculated to be 11±15 pM/s. In order to quantifying larger NO recovery and to investigate the necessary amount of NO needed to stimulate cellular migration within brain slices, different NO donors could be explored that have half-life's that fall between DETA/NO's 20 h and MAHMA/NO 60 s. A half-life in between DETA/NO and MAHMA/NO would allow more NO to be released within the 1.5 h used in the cellular migration studies. Larger NO concentration would be used to explore the influence of the concentration of NO on cellular migration. There are two possible diazeniumdiolates with shorter half-life than DETA/NO, but longer half-life than MAHMA/NO. The first is a carbon based diazeniumdiolate, p-Bisdiazeniumdiolate benzene, with a half-life of 3.6 hours.[3] The other is 1-[N-(3Aminopropyl)-N-(3-aminopropyl)]diazen-1-ium-1,2-diolate (DPTA/NO) with a reported half-life of 3 hours.[4] These diazeniumdiolate NO donors have a shorter half-life than DETA/NO, which will allow more NO to be released in the 1.5 h. The hope is that these NO release profiles obtained with these NO donor could be used to achieve a wider range of NO concentrations that are within the NO release range proposed for brain tissue to provide additional insight to the influence of NO on cellular migration in the brain.

These were the questions that I was most drawn to when thinking about the next steps in advancing this measurement method that I have developed. I hope that this system is utilized to answer many questions that are not understood presently and provide useful NO release measurements to help understanding the complex nature of NO in physiology.

4.2 References

1. Keynes, R. G.; Griffiths, C.; Garthwaite, J., Superoxide-dependent consumption of nitric oxide in biological media may confound in vitro experiments. *Biochemical Journal* **2003,** *369*, 399-406.
2. Hall, C. N.; Garthwaite, J., What is the real physiological NO concentration in vivo? *Nitric Oxide* **2009,** *21*, 92-103.
3. Arnold, E. V.; Citro, M. L.; Saavedra, E. A.; Davies, K. M.; Keefer, L. K.; Hrabie, J. A., Mechanistic insight into exclusive nitric oxide recovery from a carbon-bound diazeniumdiolate. *Nitric Oxide* **2002,** *7*, 103-108.
4. Keefer, L. K.; Nims, R. W.; Davies, K. M.; Wink, D. A., "NONOates"(1-Substituted Diazen-1-ium-1,2-diolates) as Nitric Oxide Donors: Convinent Nitric Oxide Dosage Forms. *Methods in Enzymology* **1996,** *268*, 281-293.